The Abdus Salam
International Centre for Theoretical Physics

United Nations
Educational, Scientific and
Cultural Organization

IAEA
International Atomic Energy Agency

1856-38

2007 Summer College on Plasma Physics

30 July - 24 August, 2007

On Heat Loading, Novel Divertors, and Fusion Reactors

S. M. Mahajan
University of Texas at Austin, Austin, USA

M. Kotschenreuther
University of Texas at Austin, Austin, USA

P. M. Valanju
University of Texas at Austin, Austin, USA

J. C. Wiley
University of Texas at Austin, Austin, USA

On Heat Loading, Novel Divertors, and Fusion Reactors

M. Kotschenreuther,* P. M. Valanju, S. M. Mahajan, and J. C. Wiley

Institute for Fusion Studies, The University of Texas at Austin

(Dated: November 16, 2006)

Abstract

It is shown that the limited thermal power handling capacity of the standard divertors (used in current as well as projected tokamaks) forces extremely high ($\sim 90\%$) radiation fractions f_{rad} in tokamak fusion reactors [1–3] with heating powers considerably larger than ITER-FEAT [4]. Independent of how the radiation may be apportioned between the scrape off layer (SOL) and the plasma core, such enormous values of necessary f_{rad} have serious and possibly debilitating consequences on the core confinement and stability for dependable fusion power reactor operation, especially in reactors with Internal Transport Barriers (ITBs) [5, 6].

A new class of divertors called X-divertors (XD), which considerably enhance the divertor thermal capacity through a flaring of the field lines only near the divertor plates, may be necessary and sufficient to overcome these problems and lead to a dependable fusion power reactor with acceptable economics. X-divertors will lower the bar on the necessary confinement so that routinely found H-modes [7] could be enough for a fusion reactor. A low-cost XD-based CTF that could lay the foundation for an efficient and attractive path to practical fusion power is suggested.

PACS numbers:

I. INTRODUCTION

The emergence of power exhaust as a challenging issue for the planned burning plasma experiment ITER-FEAT [4, 8–11] gives us a glimpse of the formidable heat loading problems that will pertain to an economical power producing Deuterium-Tritium (DT) fusion reactor [1–3, 12, 13] for which the heating powers are *much* larger than for ITER-FEAT. The fusion power P_F of proposed reactors lies in the range of 2500 to 3600MW [1–3, 13, 14] while the nominal P_F for ITER-FEAT is 400 MW. Consequently the reactor heating powers jump to $P_F \sim$500-1000MW, i.e. about 4-8 times larger than for ITER-FEAT. For the standard divertor configuration, the problems associated with handling such prodigious amounts of heat without destroying its components force a fusion reactor into a physical regime (characterized by a requirement for an extremely high fraction of the heating power to be radiated) very different from the one pertinent either to the current machines or to ITER-FEAT.

In order to emphasize the scope and immensity of the problem, we review in Sec.II some details of the physics and engineering of the divertor and of the scrape off layer (SOL) including its radiative capabilities. Starting with an estimate of the maximum thermal capacity of the divertor plate, we first determine how the high heat flux problem translates into requirements of high radiation fractions, and then describe the deleterious effects of such high radiation fractions on core confinement.

We find that the radiation requirements for a power reactor fitted with a standard ITER-like divertor (to be called SD) are so high that many reactor designs are arguably unworkable. Estimates based on the power levels, size, expected width of the scrape-off layer (SOL), and the likely technological limitations on a reactor divertor plate imply that the total radiation fractions (f_{rad}) must exceed 90% to save the divertor from destruction. Combining it with the ITER calculations on the maximum power that can flow into the SOL, it translates into a core radiation fraction($f_{rad-core}$) in the range of $\sim 70 - 90\%$. With such high radiative losses of the core heating power, the core confinement requirements for reactors based on advanced tokamak (AT) operating modes with high β_N and high boot bootstrap current fractions reach daunting levels. Reactors with large physical dimensions (with major radii $\sim$ 8-9 m) and very high currents $\sim$ 30 MA may be possible, but the cost of such reactors is far higher than the majority of reactor designs with major radii $\sim$ 6 m.

Our solution to the thermal exhaust problem is to modify the magnetic geometry of

the divertor. By creating an X-point near the divertor plate, the magnetic field in the open field line region is flared to increase the area over which the heat is spread. We have also demonstrated that this new configuration (called the X-divertor or XD) along with acceptable magnetic equilibria can be created with coils that may be located behind neutron shields. The desired geometry is accessible with fairly moderate currents in the additional coils. The resulting increase in the plasma-wetted area considerably reduces the amount of required radiation before the thermal flux is incident on the divertor plate. The X-divertor, described and explained in Sec.III, brings the required radiation fraction (for a high power reactor) much closer to the range where ITER-FEAT is expected to operate.

We would like to stress here that numerically computed magnetohydrodynamic (MHD) free boundary equilibria, with XD-coils, show that the magnetic flux can be greatly expanded near the divertor plate without affecting the capability to create highly shaped equilibria with high elongation and triangularity. Small non-axisymmetric coils are used to circumvent undesirable linkings (with PF coils inside the TF coils); the ripple produced by non-axisymmetric coils turns out to be acceptably small. With XD-coils, the magnetic flux expansion may be increased by up to an order of magnitiude compared to the standard geometry, while simultaneously increasing the field line length by a factor of two or more. It is impossible to obtain this combination with the standard divertor geometry.

We are aware that the X-divertor can become a serious reactor candidate only if relatively simpler and traditional mechanisms fail to solve the exhaust problem. If one could radiate, for instance, substantial fraction of the thermal power without affecting the stability and confinement of the core plasma, a "radiation solution" will be ideal.

A thorough examination of the possible "radiation solutions" constitutes the subject matter of Sec.IV and Sec.V. In the former we concentrate on the H-mode while the latter is devoted to the Internal Transport Barrier (ITB) mode of operation. The reactor applicability of various strategies that increase SOL impurity radiation without affecting the core confinement (and which have been successful in present experiments) is examined. One-D fluid models of the SOL, which clarify many basic physical processes, have been our principal tool. Several dimensionless parameters are identified which relate to the capability of a divertor SOL to radiate power. All these parameters have a rather unfavorable scaling with parallel heat flux even for effects such as parallel heat convection and impurity entrainment. The upshot of this is that a large increase in the impurity level in the SOL results in a

remarkably small increase in the allowable power into the SOL. For high powers into the SOL, it is not possible to radiate a large fraction of the SOL power. The severe implication is that the power must be radiated in the core.

Two dimensional simulations using UEDGE are used to quantify our findings. The 2D runs confirm the qualitative trends in the 1D results. The 1D results are important, however, because they show that the unfavorable scaling of SOL radiation is based on the characteristics of transport parallel to field lines. Parallel transport in the SOL is fairly well understood, whereas the perpendicular transport is not so. Simulations in 2D must inevitably make assumptions about the perpendicular transport. Since the unfavorable scaling of SOL radiation is shown to be dictated by the nature of parallel transport, the result has a significantly more robust physics basis than what can be provided by 2D simulations alone.

For a device the size of ITER-FEAT, a heating power of $\sim$100 MW is expected to be close to the limit of the power handling capability of a standard divertor, even with substantially increased impurity levels (as long as full detachment is avoided - as planned for ITER). We will show later that increasing the level of impurities to raise SOL radiation results primarily in increased core radiation rather than higher SOL radiation.

Another experimental strategy examined here is the idea of a "radiating mantle" where core radiation is primarily limited to the far edge of the plasma so that confinement degradation might be avoided. This strategy would work if one could arrange the radation power densities in the edge to be much higher than in the core. However, in section IV, we show that this strategy has an unfavorable scaling with temperature and with $n\tau_P$ (the product of the density and the particle confinement time). For reactor parameters with an H-mode edge, the core radiation cannot be isolated very near the edge; it ends up pervading the entire core. For plasma profiles for AT operation with high beta, high bootstrap fraction and an ITB, a large majority of the radiation, again, comes from inside the ITB. Thus the "radiating mantle" strategy fails in both of the projected modes of reactor operation. Attempts to radiate primarily in a mantle end up radiating most of the power in the core.

In addition to raising the bar on core confinement, high ($f_{rad-core}$) is harmful in several other ways. In Sec.VI, for instnace, we show that a self-heated fusion plasma is thermally unstable in the presence of a high core radiation fraction $f_{rad-core}$. At high $f_{rad-core}$ forced by the standard divertor (SD), the thermal instability is sufficiently virulent that feedback methods appear unworkable for ITB plasmas. Virulent thermal instabilities quite probably

must be avoided for a reliable power reactor.

Since $f_{rad-core}$ erodes the core heating power and hence implies that the core transport must be reduced, the resulting inadequate helium exhaust will cause a radiation collapse of the core inside the ITB. This phenomenon is discussed in Sec.VII.

Having failed to find a radiation solution, the challenge of reducing f_{rad} down to a manageable level reverts to the X-divertor. Note that liquid metal divertors [15–17] with a higher heat flux capacity may also be used. The liquid metal divertors are fully compatible with, and, in fact, are enabled by the weaker poloidal fields in the XD-geometries.

Clearly, the new X-divertor (XD) needs to be subjected to rigorous experimental tests before implementation in a reactor. In fact, there is a fortunate symbiosis between the proposed X-divertor (XD) concept and a Component Test Facility (CTF) [18] (discussed in some detail in Appendix A). A CTF is recognized as a critical step for developing the fusion technology necessary for a reactor. It is shown in Appendix A that a CTF is not possible with a standard divertor (SD), but will become possible with the new X-divertor (XD). A CTF-XD can also play a critical role in the physics development of fusion by demonstrating the workability of new X-divertor under reactor-like conditions. If the new X-divertor does what it is expected to do, it will be relatively straightforward to scale a CTF-XD to a reactor.

In Sec.VII, we sum up our findings including our suggestions for future experiments.

II. REACTOR POWER HANDLING LIMITS - HIGH RADIATION FRACTION

In this section we set up the necessary preliminaries for exploring the radiation strategies. The first order of business is to estimate the radiation fraction f_{rad} required to avoid damage to the divertor plate. The material and engineering constraints, under reactor conditions, set a stringent upper bound on the heat flux (q_{max}) that can hit the divertor plate. A reactor divertor, with a minimum lifetime of one to two years, will be exposed to high power bombardment for times that are about two orders of magnitude longer than the duration over which an ITER divertor is expected to operate. Due to the extended exposure, it will accumulate roughly two orders of magnitude greater neutron damage than the ITER divertor. Hence the upper limit on q_{max} for a reactor divertor could be, at best, comparable to that of ITER [1, 13, 19, 20]. We will assume in what follows that the divertor heat flux problem is not likely to be solved merely by technological improvements in the divertor plate

Device Name Divertor: SD/XD	**Heating Power** P [MW]	**Major Radius** R [m]	P_{heat}/R [MW/m]	P_{heat}/R^3 [MW/m^3]
DIII-D	10	1.6	6	-
JET	17	3.	6	-
JT-60U	17	3.4	5	-
ITER-FEAT	120	6.2	19	0.5
ITER-EDA	300	8.2	37	0.5
EU-A	1246	9.6	130	1.4
EU-B	990	8.6	115	1.6
EU-C	792	7.5	106	1.9
EU-D	571	6.1	94	2.5
ARIES-AT	387	5.2	74	2.8
ARIES-RS	515	5.5	94	3.1
Slim-CS	645	5.5	117	3.9
CREST	691	5.4	128	4.4

TABLE I: Values of (P_{heat}/R) and (P_{heat}/R^3) for 3 current experiments, 2 proposed burning plasma experiments (BPX), and 8 proposed reactors

properties, and q_{max} will be taken to be 10 MW/m^2 in this paper.

A commonly used metric (derived for constant SOL width) for the divertor heat loading is P_{heat}/R. Recent results from B2-Eirene simulations [21, 22], however, suggest that P/R^3 is a more appropriate metric for devices on the scale of burning plasmas or reactors (but not smaller experiments - further discussion in section IV). In Table I we compare both these metrics for some existing machines, ITER, and various proposed reactors. Both measures of heat-loading are much higher for reactors than for ITER.

Extensive analysis of the ITER divertor indicates that it is within a factor of about 1.4 from the limit of power handling capabilities with about 86 MW going into the SOL (with q_{max}=10 MW/m^2).Since reactors have much higher levels of P_{heat}/R (or P_{heat}/R^3), the power entering the SOL would have to be reduced by addition of impurities to produce core radiation.

In Table II, we show what $f_{rad-core}$ will be needed for reactors (including ITER) if we

Device Name Reactor/BPX Divertor: SD/XD	$f_{rad-core}$ **to give same** P_{SOL}/R **as ITER-FEAT (SD)**	$f_{rad-core}$ **to give same** P_{SOL}/R^3 **as ITER-FEAT (SD)**	$f_{rad-core}$ **with** P_{SOL}/R **metric if XD is used**
ITER-FEAT	16%	16%	
ITER-EDA	56%	22%	
EU-A	88%	70%	69%
EU-B	86%	73%	65%
EU-C	85%	78%	62%
EU-D	83%	83%	57%
ARIES-AT	78%	85%	46%
ARIES-RS	83%	86%	57%
Slim-CS	86%	89%	66%
CREST	87%	90%	68%

TABLE II: Necessary core radiation fractions to obtain the same values of P_{SOL}/R and P_{SOL}/R^3 as for ITER-FEAT, and values of the core radiation fraction using the XD and the P/R metric.

assume that the entire class has the same P_{SOL}/R (or P_{SOL}/R^3) as ITER, which with $P_{SOL} = 100$ MW and $R = 6.2$ m, provides the baseline reference. One can again notice the stark contrast between ITER and all other reactors; for the latter the core radiation fractions are in the range ∼70-90%, reaching 78-90% for the more attractive advanced tokamak (AT) mode reactors. Such core fractions are far higher than on almost all present experiments operating AT modes. For either H or AT modes, ITER-FEAT is not expected to be able to operate as a burning plasma for $f_{rad-core}$∼70-90%. In this important sense, reactors are in a regime which cannot be tested on ITER-FEAT. As we shall see, important phenomena like thermal instability and helium exhaust depend strongly on $f_{rad-core}$.

Table II also shows that the required $f_{rad-core}$ is substantially reduced with XD.

High $f_{rad-core}$ naturally erodes the core heating power. Taking P_{net}=$P_{heat}(1 - f_{rad-core})$ as an estimate for the net heating power, the confinement requirements for the reactors are shown in Fig.1. where we also display the confinement range of present experiments. If the allowable power into the SOL scales as R^3, the H-mode reactors require a modest improvement over conventional H-modes - an enhancement by a factor of about 1.2 relative

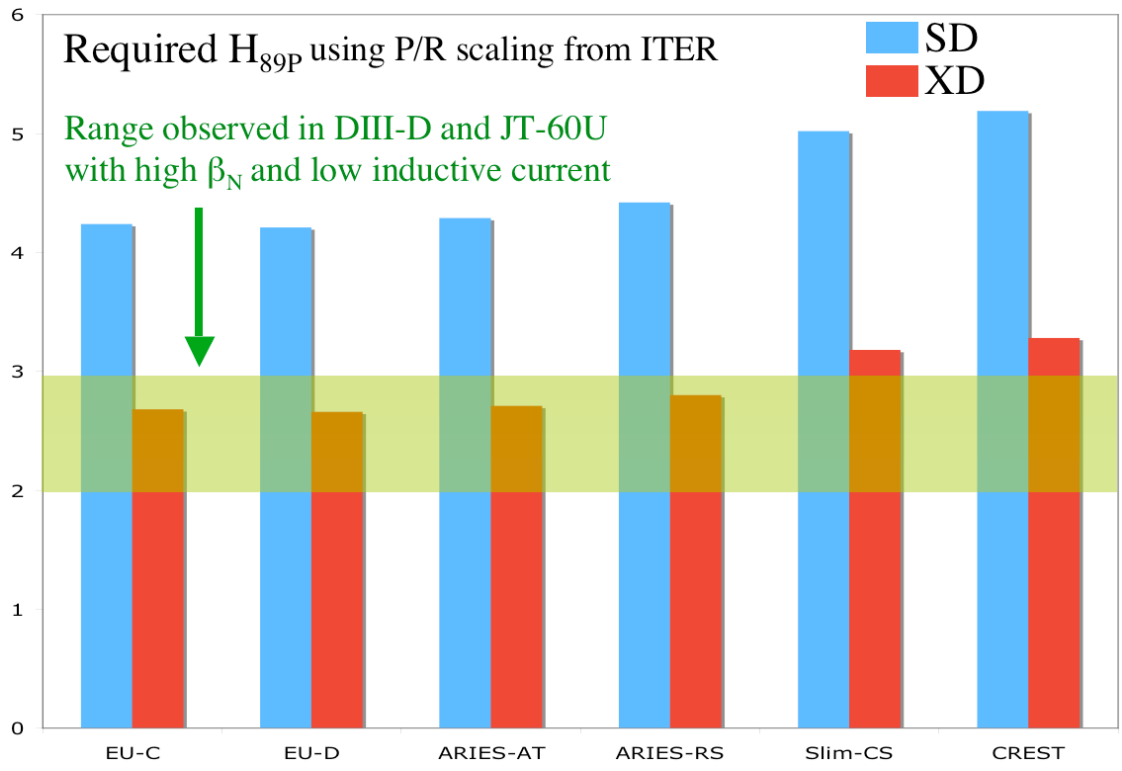

FIG. 1: Confinement requirements for reactors as compared to the confinement range achieved on present experiments. The net heating power is estimated to be P_{net}=$P_{heat}(1 - f_{rad-core})$.

to the ITER98H(y,2) scaling law. For AT reactors, on the other hand, the confinement enhancements (over present experiments in similar operating modes) have to be much larger. (We use results reported from DIII-D and JT-60U which are closest to reactor conditions - values of β_N which are the largest achieved with low inductive current. For DIII-D the parameters are $\beta_N = 4$ with H89P= 2.5 [23], and for JT-60U, the parameters are $\beta_N = 2.5-3$ with H89P = 2.9-2.1 [24, 25].) We draw the reader's attention to another feature of Fig.1: for reactors using the X-divertor, the radiation fractions are brought down to the range of present experiments (further discussion in section IV).

Inventing or exploring mechanisms to increase allowable power into the SOL, particularly for reactors operating in the AT mode, would strongly lower the confinement bar. For a standard divertor, the two common methods of increasing P_{SOL} are: 1) to increase density, and 2) to increase impurities. Results from B2-Eirene [21, 22] for ITER-FEAT show that, when operating at the highest density possible before full detachment, P_{SOL} is limited to 125 MW if the peak heat flux on the divertor plate were not to exceed 10 MW/m^2. To allow

enough margin for reliable divertor operation in a practical reactor, 100 MW as an upper bound for an ITER sized reactor (as used in Fig.1) seems reasonable; UEDGE yields similar results.

When experiments proceed beyond partial plasma detachment to full detachment, divertor heat fluxes are greatly reduced and radiation levels become higher. Full detachment, however, is accompanied by consequences that are broadly and deeply discouraging. Experiments show that full detachment leads to: 1) very poor H-mode confinement (closer to L-mode), or 2) total loss of H-mode, and 3) high disruptivity. In Appendix B, some of the experimental evidence is breifly reviewed. Here we simply note that full detachment is not regarded as a viable regime for ITER [8, 26].

The remaining option to elevate P_{SOL} "via impurities" is examined In section IV. We find that higher levels of impurities have a surprisingly small impact on the maximum P_{SOL}. Although we must wait for Secs. IV and V for building a convincing case, we mention here that our search has failed to find any acceptable and attractive "radiation solution".

We are thus led to seek divertor innovations that modify the magnetic geometry. The X-divertor, discussed in Sec.III, is the most promising result of this effort.

We end this section by transforming Table II (based on $f_{rad-core}$) to Table III to conform to a common experimental custom of using the total radiation fraction f_{rad} (including radiation power in the core, the SOL and the divertor). The total amount of power that can fall on the outboard divertor plate P_{plate} is the product of the plasma-wetted area A_w and the maximum heat flux q_{max} =10MW/m^2. The wetted area is estimated by [27]

$$A_w = \frac{2\pi R}{\sin(\theta_t)} W_{SOL} F_{exp} \tag{1}$$

where W_{SOL} is the width of the SOL at the midplane, F_{exp} is the flux expansion, and θ_t is the angle between the plate and the poloidal field. The "power" scrape off layer width can be estimated by various means. For parameters of ITER and reactors it yields values in the range of 1/2-1 cm. To draw Table III we invoke: 1) the most optimistic value W_{SOL}=1 cm to maximize the plate area, 2) the divertor angle (θ_t=25 degrees) to be the same as for ITER-FEAT, and 3) the maximum divertor heat flux q_{max}= 10MW/m^2 [1, 13, 19, 20].

The first two columns in Table III show that P_{plate} is much less than the heating power for all reactors. Most of the heating power, therefore, must be radiated. Experiments find that a larger fraction of the power falls on the outboard than the inboard divertor [28].

Device Name **Divertor: SD/XD**	P_{plate}	P_{heat}	**Total** f_{rad} **with SD**	**Total** f_{rad} **with XD**
ITER-FEAT	37	120	54%	
ITER-EDA	48	300	76%	
EU-A	57	1246	93%	66%
EU-B	51	990	92%	61%
EU-C	45	792	92%	58%
EU-D	36	571	90%	52%
ARIES-AT	31	387	88%	40%
ARIES-RS	33	515	90%	52%
Slim-CS	33	645	92%	62%
CREST	32	691	93%	65%

TABLE III: Estimated total radiation fractions f_{rad} necessary to limit the divertor heat flux to 10 MW/m^2 for the standard (SD) and X-divertors (XD).

Using a representative value of 2/3 for the fraction of power falling on the outboard divertor $f_{Outboard}$ (1/3 of the power falls on the inboard), the total radiation fraction

$$f_{rad} = 1 - P_{plate}/(P_{heat} f_{Outboard}) \tag{2}$$

for the proposed reactors (shown in Table III) come out to be typically $> 90\%$. On present experiments, such high radiation fractions are strongly associated with confinement deterioration and enhanced disruption probability.

III. NEW DIVERTORS - INCREASED HEAT FLUX CAPABILITY

In the preceding sections we have shown that the divertor is the key element in the thermal architecture of a fusion reactor and that the limited heat-rating of the standard divertors (SD) makes it extremely difficult to find a reactor-relevant operating regime. In Sec.II we also demonstrated that the XD devices, with new X-Divertors whose heat-handling capacity is much higher than the SD devices, can relatively easily fulfill the confinement and other demands for a high power fusion reactor. This section is devoted to a detailed discussion of the concept and feasibility of this new X-divertor (XD).

The new divertors [29, 30] will be able to conservatively allow 2.5 times more power into SOL as compared to the standard, optimized ITER-like divertors [8]. The high power rating is brought about by big increases in the plasma-wetted area through small but carefully designed changes in the poloidal magnetic field in the divertor region.

The obvious first step is to try to increase the plasma-wetted area on the divertor plate by tilting the plates to decrease the poloidal strike angle. This is a standard optimization practice and the power limits on the standard divertors quoted in this paper had already been subjected to tilt optimization. However, for tilt angles less than about 25 degrees, this technique yields little improvement [31] or no improvement [32] in power handling. The novel divertors can and do use the standard optimizing methods, but the main source of their large gain is due to a fundamental change in the magnetic geometry of the divertor region. The main results from [29, 30] are summarized here.

The basic idea behind the new X-divertors (XD, Fig.2) is to flare the field lines downstream from the main plasma X-point. As shown in Fig.2, while field lines converge as they move downstream from the X-point in a standard divertor (SD), they can be made to diverge by creating another X-point near the divertor plate. This extra downstream X-point can be created with an extra pair of poloidal coils (dipole: with opposing currents). Each divertor leg (inside and outside) needs such a pair of coils.

For a reactor, this would entail linked coils. This can be avoided in many ways. De-mountable TF coils, enabled by high TC superconductors, can provide a solution. Even de-mountable PF coils (used for the XD coils) inside non de-mountable TF coils will work. Each XD coil carries about a third of the current in a TF coil, so de-mountable XD coils would presumably be considerably easier than de-mountable TF coils.

In addition, the axisymmetric coils can be replaced with smaller modular coils that produce the same axisymmetric field components (Fig.2). We have shown that the non-axisymmetric ripple for this configuration is small in the core plasma ($< 0.3\%$ at the plasma x-point, and far smaller than the ripple due to the TF coils inside the core plasma). The distant main plasma is hardly effected because the line flaring happens only near the extra coils. In this respect, these X-divertors (XD) are completely different from the old bundle divertors which created a large ripple in the main plasma. Since one needs to cancel only the small poloidal field at the new X-point, the corresponding coil currents are small. With the modular PF coils, the non-axisymmetric variation in the normal magnetic field at the

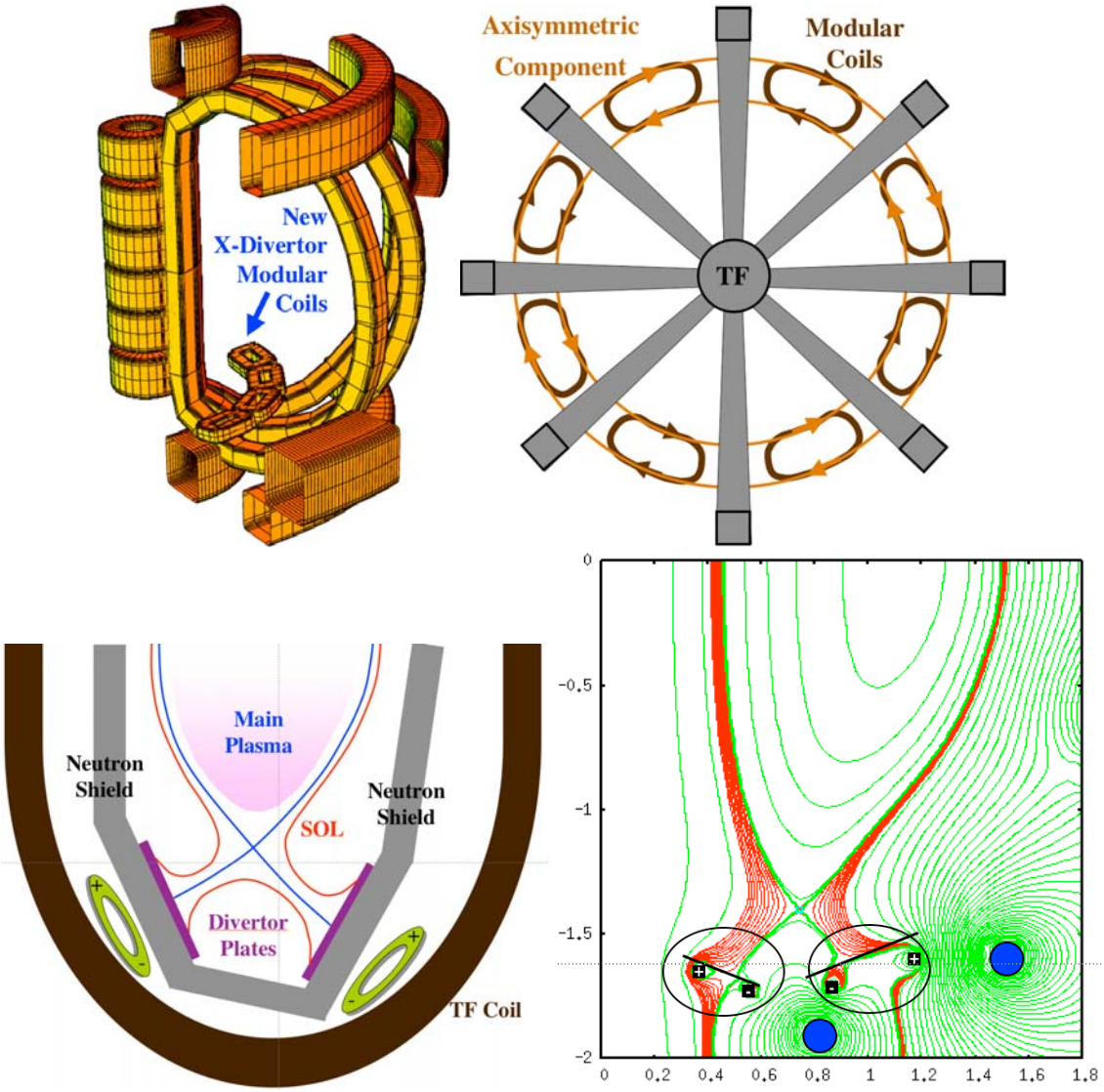

FIG. 2: Top left: Modular X-divertor (XD) coil loops (which can be rectangular). Note that the plasma *does not go through the loops* - the loops are behind the divertor plates (these are not bundle divertors). Top right: The axi-symmetric component of the currents in the loops is equivalent to the axisymmetric poloidal coils (+ and −) with opposite currents. Only 8 TF coils are shown in this top view for clarity. Bottom left: Side view. Modular coils are behind neutron shield. Bottom right: Flux expansion (see encircled areas) in NSTX MHD equilibrium.

divertor plate would be large enough to cause "hot spots" on an axi-symmetric divertor plate. There are two remedies to this. The simplest is to slightly ripple the divertor plate to follow the rippled magnetic field. The normal component of the field can then be made

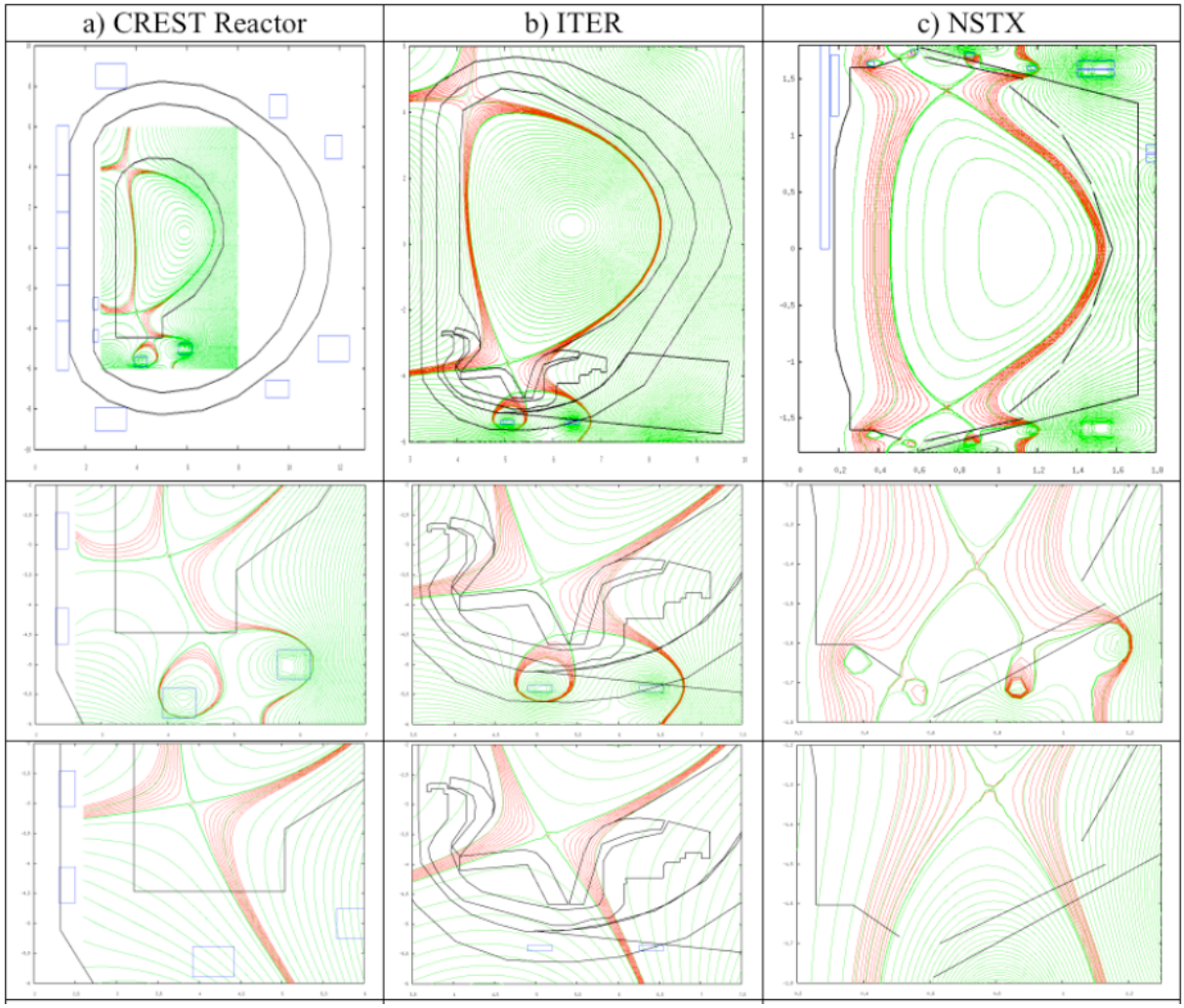

FIG. 3: New X-divertor (XD) equilibria for Left: CREST Reactor, Middle: ITER, and Right: NSTX. In each column, the second and third rows show the large flux expansion near the divertor plate when the new small coils are turned on and off respectively. For CREST and ITER, the coils are behind neutron shield. For ITER, coils can be designed to be inside divertor cassettes.

constant (for any given current in the modular coils). Also, it is possible to keep the divertor plate axi-symmetric, but add correction coils which create a canceling oscillation in the normal component of B, so that the normal component of B is constant to within about 10% near the strike point. These correction coils increase the number of ampere turns in the XD related coils by about a factor of two compared to the modular coils alone.

The gain in the plasma wetted area can be very large (5 or more), as shown in Figs.2-3 and in Table IV. The reduction in poloidal field also increases the line length by ∼2-3 times.

Device	**Divertor**	Flux expansion	L_{XT} (X to Target)	Ratio L_{XT}/L_{XM}
NSTX	Standard (SD)	2.3	5.3 m	0.29
	New X-div (XD)	20.4	6.9 m	0.32
ITER	Standard (SD)	4.3	23 m	0.45
	New X-div (XD)	22.7	65 m	1.12
CREST	Standard (SD)	3.3	37 m	0.74
	New X-div (XD)	23	75 m	1.19

TABLE IV: SOL field line parameters of 3 equilibria obtained with FBEQ [33].

This will better isolate the plasma from the divertor plate in the parallel direction. Impurity entrainment should be considerably enhanced, leading to better radiation capability and reduced impurity levels in the main plasma. Also, the plasma temperature at the plate can be substantially reduced, leading to less plate erosion and impurity generation. An additional advantage is that it is easier to attain main plasma configurations of high triangularity (even inside indentation), high elongation, and high or low poloidal beta. Such configurations have very beneficial MHD implications.

The extra X-divertor (XD) coils could possibly be accommodated in an existing machine, or in a reactor with a modest increase in the complexity of the magnetic design and a very small increase in toroidal field volume. Although a design with the modular coils in the removable ITER divertor cassette is magnetically feasible (see Fig.2), practical engineering problems will probably prevent any such retrofit for ITER. However, this "conceptual design" exercise demonstrates the feasibility of using modular copper coils behind less shielding than superconducting coils for a reactor. Alternatively, their location can be behind the blanket and shield so that superconducting coils may be used, as in the CREST design. In summary, the small modular coils are reactor-relevant. Their positive impact on divertor performance can be large, while their negative impact on the main plasma (ripple) can be very small.

The five-fold flux expansion increases the divertor power handling capability, and thus lowers the fraction of power that must be radiated in the core or in the SOL. By drastically reducing the large core radiation required to save the divertor, the XD may become the key to overcoming the major roadblock in our march to higher power fusion reactors.

The primary advantage of the XD for core plasma physics arises from the increase in P_{SOL}

which it enables. However, if the XD increases the flux expansion by a factor of 5, P_{SOL} increases by less than a factor of 5. This occurs because of the reduction in the radiation fraction which occurs at high $Q_{||}$. Using the extended model, the ratio of P_{SOL}(XD) to P_{SOL}(SD) is expected to be roughly 3 for similar conditions. The SOL radiation fraction for ITER power levels is $\sim 50\%$ for the SD. Making the pessimistic assumption that there is negligible radiation for the XD, then the XD increases P_{SOL} by a factor of 2.5. This is the factor which has been used in creating Table II.

Because of this, the core confinement requirements on the reactor plasma are substantially reduced - to a range which is within the present operating experience.

IV. SOL RADIATION

In Sec.III, we presented a "magnetic solution" to the reactor heat flux problem. Although appropriate coils can be readily designed for the X-divertor, it still constitutes a non-trivial change to be undertaken only if relatively simpler solutions are not available or adequate. This section explores what we call the radiation option. Remembering that our principal goal is to minimize the core radiation fraction so that there is enough core confinement for the generation of fusion energy, the success of the radiation option will depend on our ability to find effective non-core avenues for radiation. The SOL, and a small radiating mantle at the plasma edge are the two principal avenues that we now investigate.

Considerable experimental effort has been spent in attempts to radiate a large fraction of the power going into the SOL. In some cases, quite large fractions of P_{SOL} have been radiated[34–37]. One could get very encouraged from the current experimental success till one asks the question - can these results be extrapolated to reactors which lie in a totally different regime of heating power?

To study the scaling of radiation losses in the SOL, we use 1D as well as a 2D models. The 1D models are useful in elucidating the underlying physics. For quantitatively dependable results, we turn to 2D models. We note that the 2D models suffer from a basic shortcoming; they must make assumptions about perpendicular transport because perpendicular transport is not well understood. The 1D models, on the other hand yield results that are fundamentally dictated by parallel transport, which is relatively well understood. One then expects that a 1D model with adequate physics will capture the salient qualitative

features (like scaling of radiation with with power) of the SOL dynamics quite well.

The principal result of this part of the enquiry is that maximum attainable radiation fraction in the SOL scales unfavorably to reactor parameters. With the standard divertor, therefore, the required $f_{rad-core}$ remains too high for comfort.

One dimensional (1D) models have long been used for divertors [27]. In the early design phase of ITER, the potential radiation losses in the SOL were estimated through such models. Experiments on DIII-D found that two additional effects could substantially increase the SOL radiation - the parallel convection and impurity entrainment. The investigation presented here show that even when these these effects are included, the radiation fraction in the SOL scales very unfavorably to systems with high parallel upstream heat flux $Q^u_{||}$. In the range of smaller $Q^u_{||}$ peculiar to present experiments, large radiation fractions are possible in the SOL. Unfortunately, as we extend $Q^u_{||}$ to the range of ITER-FEAT, and beyond ITER-FEAT to reactors, the attainable SOL radiation fraction decreases considerably. The adverse scaling greatly limits the power that can be radiated in the SOL. This does not bode well for it is precisely when $Q^u_{||}$ is large that larger radiation fractions are needed to maintain the heat flux on the plate below the tolerable maximum q_{max}.

The 1D analysis presented here also shows that greatly increasing the level of impurities is remarkably ineffective at increasing the radiation fraction in the SOL. The one dimensional models are useful for highlighting that the underlying physics for these results stems from the basic properties of parallel transport and impurity radiation.

The 1D results are found to be quite similar to UEDGE calculations, but UEDGE results are somewhat more optimistic. It is also found that quantitative agreement with UEDGE is greatly improved by allowing for different electron and ion temperatures, which has rarely been done in the past for 1D models. Hence, results from a 1D model with separate equations for electron and ion temperature are also presented (together with classical equilibration). UEDGE results, similar to the 1D model, also show that even large increases in impurity levels in the SOL do not greatly increase the allowable P_{SOL}. The conclusion is that increasing the impurity level results in only marginal increases in the SOL radiation. Attempts to increase SOL radiation by substantially increasing impurity levels simply ends up in a large increase in the core radiation; the divertor heat loads can, therefore, be kept low only if the core bears the brunt of the radiation requirements.

A. Scaling paramters from a basic 1D divertor model

The strategy of preferentially enhancing divertor radiation (without affecting the core) with impurities has been used with some success in present experiments [35, 36]. We now exploit 1D models of the divertor to examine the scaling of this strategy to high power levels. Let us begin with a 1D model where the electron and ion temperatures are assumed to be equal. (This simplifying restriction will be relaxed shortly). The heat conduction is determined by classical electron thermal conduction and parallel convection[27].

$$Q_{||} = \kappa_0 T^{5/2} dT/dl + 5unT + mu^3/2 \tag{3}$$

where u is the convection velocity, l is the distance along the field line, and n and T are respectively the density and the temperature. The heat flux is reduced by: 1) impurity radiation from a given fraction of impurities f_z radiating with a characteristic radiation rate L_z, and 2) hydrogenic ionization radiation R_H,

$$dQ_{||}/dl = f_z n^2 L_z(T) + R_H \tag{4}$$

We first derive some pertinent dimensionless parameters from these equations, and compare the values of these parameters for some present experiments with ITER and reactors.

In the simplest 1D model for impurity radiation, convection and hydrogen radiation[38] are ignored. This will be referred to as the basic model. The basic model is known to underestimate radiation, but it provides a useful point of departure; it also allows the construction of dimensionless parameters that are simple and easily evaluated. More complete 1D models and 2D UEDGE simulations confirm the trends implied by these dimensionless parameters. In the basic model, the density along the field line is evaluated using pressure balance,

$$nT = n_u T_u \tag{5}$$

where n_u (T_u) is the upstream electron density (temperature). The basic model can then be solved analytically in terms of an intergral over T[38],

$$\frac{Q_{||u}^2 - Q_{||p}^2}{2} = f_z n_{eu}^2 \int L_z(T) T^{1/2} dT \sim f_z n_{eu}^2 L_z(T_{rad}) T_{rad}^{3/2} \tag{6}$$

In the last equation, the temperature integral is approximated in terms of T_{rad} = the temperature at which the radiation is maximum. The solution is valid for $T_u >> T_{rad}$ and

$T_p << T_{rad}$ where T_p is the electron temperature at the plate. The upstream electron temperature can be estimated in the conduction limited regime [27]

$$T_{eu}^{7/2} = \frac{7Q_{||u}L}{2\kappa_0} \tag{7}$$

where L is the total line length. The radiation fraction $f_{rad-SOL}$ is equal to the fraction of $Q_{||}$ which is removed by radiation, $(Q_{||u} - Q_{||p})/Q_{||u}$. A simple dimensionless measure F of $f_{rad-SOL}$ can now be defined by using eq(6) and the approximation for small radiation fractions $Q_{||u}^2 - Q_{||p}^2 \sim (Q_{||u} - Q_{||p})Q_{||u} \sim f_{rad-SOL}Q_{||u}^2$,

$$F = \frac{7^{4/7}\kappa_0^{3/7} f_z n_{eu}^2 L_z(T_{rad}) T_{rad}^{3/2} L^{4/7}}{2^{4/7} Q_{||u}^{10/7}} \tag{8}$$

The dimensionless parameter F serves as a figure of merit for the radiative ability of the SOL. For a given impurity density, F strongly decreases with input power, and mildly increases with line length. This is true for all impurity densities. Representative values of F, computed for present experiments, ITER and reactors, are exhibited in Table V. We have assumed that the core radiation fraction of the reactor is 50%, so that half of the heating power goes into P_{SOL}. It is strikingly obvious that this simple dimensionless estimate of the SOL radiation fraction is much lower for reactors than for present experiments or ITER.

The basic model, devoid of several important mechanisms, is known to underestimate the radiation in the SOL. One of these mechanisms is parallel convection- experiments on DIII-D found that convection can be the dominant energy transport process at low temperatures where radiation is most copious [34]. Parallel convection increases the energy transport along the field line above the basic model, so that the temperature in the radiating region does not decrease as rapidly through the temperature of maximum radiation. The resulting increase in the length of the radiating zone along the field line increases the total radiation. The potential importance of convection at the maximum radiating temperature can be gauged as follows. Since the maximum attainable value of the parallel flow is approximately the sound speed $v_s = (2T_{rad}/m_i)^{1/2}$, the maximum parallel heat flux that can be carried by convection is roughly $6nT_{rad}v_s$. The ratio C

$$C = \frac{67^(2/7) n_{e0} T_{rad} v_s L^{2/7}}{2^{2/7}\kappa_0^{2/7} Q_{||u}^{5/7}} \tag{9}$$

between the maximum convective, and the upstream heat flux provides us another dimensionless parameter of significance. In the definition of C we have used eq.5 and eq.7 to eliminate n_e in terms of the upstream density n_{eo}.

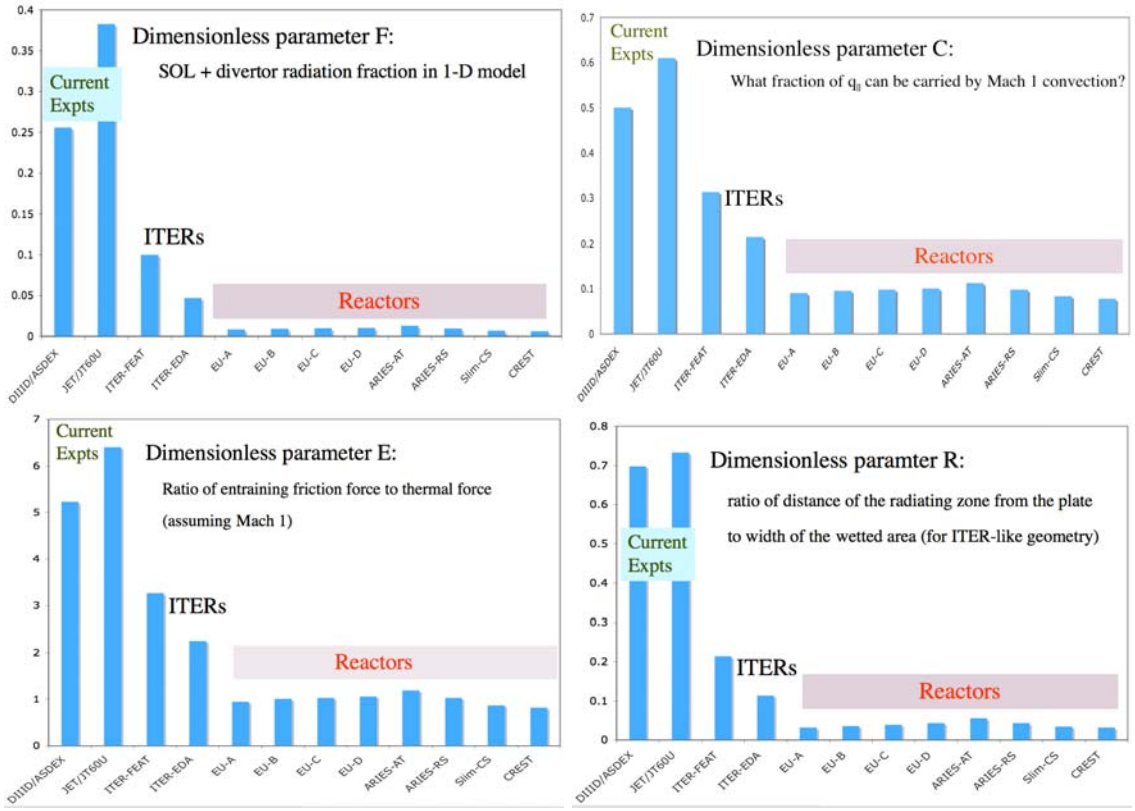

FIG. 4: Dimensionless figures of merit F, C, E, R from 1D model.

Values of C in Table V again tell us that for reactors, in direct contrast to DIII-D, convection cannot substantially increase the radiation above the basic model.

Another dimensionless parameter of a geometric nature, measuring the effectiveness of radiation for preventing the heat falling on the plate, is also readily constructed. If the radiation occurs very close to the plate, then roughly half the radiation can fall on the plate in essentially the same position where the plasma hits the plate. At constant parallel heat flux $Q^u_{||}$, the temperature in the basic model varies as $T^{7/2} - T^{7/2}_{plate} = (2/7)lQ^u_{||}$, l being the distance from the plate . Neglecting T_{plate} for simplicity (typically it is small), we obtain an estimate for the distance L_{rad}(from the plate) at which the radiation occurs,

$$L_{rad} = \frac{2T^{7/2}_{rad}}{7\kappa_0 Q_{||u}} \tag{10}$$

This distance is to be compared with the width of the wetted area on the plate $W_{wetted} = W_{SOL}F_{exp}/\sin(\theta_t)$ estimated in analogy with eq.1. We now define R to be the dimensionless

Device Name	F	C	R	E
DIII-D	0.26	0.61	0.7	5.2
JET	0.38	0.5	0.7	6.4
ITER-FEAT	0.10	0.31	0.21	3.3
ITER-EDA	0.047	0.22	0.11	2.2
EU-A	0.008	0.09	0.03	0.9
EU-B	0.009	0.1	0.04	1.0
EU-C	0.009	0.1	0.04	1.0
EU-D	0.010	0.1	0.04	1.1
ARIES-AT	0.013	0.1	0.05	1.2
ARIES-RS	0.010	0.1	0.04	1.0
Slim-CS	0.007	0.08	0.04	0.9
CREST	0.006	0.08	0.03	0.8

TABLE V: Values of dimensionless parameters F,C,R and E for experiments, proposed burning plasma experiments and reactors

ratio of the distance from the plate to the width of the wetted area

$$R = \frac{L_{rad}\sin(\theta_t)}{W_{SOL}F_{exp}} \tag{11}$$

If this ratio is large, the radiation is well dispersed away from the wetted area on the plate. But for R much less than one, half of the radiation will fall on the plate in the region wetted by the plasma, significantly reducing the effectiveness of radiation as a means of reducing the heat flux. Values of R, displayed Table V, clearly reveal that, for reactors, a substantial fraction of the radiation will fall back on the plate.

Finally, the impurity fraction f_z need not be constant along a field line. Impurities can be entrained by the divertor flow to concentrate near the plate, and thus increase the divertor radiation without increasing the impurity concentration in the core[35]. The plasma flow to the plate causes a friction force on the impurities toward the plate, whereas the thermal force tends to drive impurities away from the plate. At the temperature T_{rad},

$$E = \frac{m_i v_s}{\tau_s(\alpha_e + \beta_i)dT/dl} \tag{12}$$

is the ratio of these forces, where the values of the coefficients can be found in references [27, 39]. To define E, the flow in the radiating zone has been taken to be Mach one (roughly the maximum possible). If E is much greater than one, there is substantial potential for impurity entrainment. The values of E for current experiments, ITER and reactors are listed in Table V. The usual story is repeated - the potential for impurity entrainment is significantly lower in reactors than in present experiments or ITER.

The basic 1D model is simple enough to allow direct and instructive comparisons of gross physical effects, find their trends, and to clarify their origins. However, it is known to substantially underestimate the radiation predicted in 2D models. The agreement of 1D models with 2D models is considerably improved by including convection and by allowing unequal electron and ion temperatures. Numerical analysis of this more complete 1D model shows all the same trends as in the basic model. This is described below.

B. Extended 1D model

Though the basic model is instructive, more complete 2D models show that more power can be dissipated in the SOL. In this section, a more complete 1D model is presented which gives results in roughly the same range as the 2D models. This model also displays the trends described in the preceding subsection. The fact that such a 1D model gives results fairly close to the 2D simulations gives confidence that it captures the principal and crucial aspects of the relevant physics. Thus, the unfavorable scaling of SOL radiation with parallel heat flux for reactor regimes appears to be a consequence of parallel transport in the SOL. Since parallel transport in SOL is dominant and well understood, the trend has a sound physics basis. While 2D models are more complete, they too have to make assumptions about the perpendicular transport which is much less understood.

The extended model contains separate equations for the electrons and ions, with each species having the appropriate parallel energy transport. The convection is included parametrically, as a specified functional form which is similar to that found in UEDGE runs. The convection is concentrated near the divertor plate, and the amount of its extension upwind is varied to produce the maximum power dissipation. Appropriate sheath boundary conditions are used at the plate. The detailed equations are found in Appendix C. This model will be referred to as the extended 1D model.

Device Name	$Q_{\|\|u}$ **in GW/m**^{2}
ITER-FEAT	.34
ITER-EDA	.64
EU-A	2.3
EU-B	2.0
EU-C	1.9
EU-D	1.7
ARIES-AT	1.3
ARIES-RS	1.7
Slim-CS	2.1
CREST	2.3

TABLE VI: Estimated values of $Q_{||u}$ for different devices assuming 50% core radiation fraction, based upon the analysis in section II.

This model is solved numerically and compared to the basic model and UEDGE for reactor parameters. A fixed fraction of Ne equal to 1% is assumed, and the radiation fraction is computed as $Q_{||u}$ is varied. (The geometry and parameters are similar to ITER - see Appendix C. The extended model gives results in much closer agreement to UEDGE than the basic model. However, all trends remain the same as in the basic model.

In order for the standard divertor plate to survive, the radiation fraction must be increased as the parallel heat flux is increased. However, the opposite occurs in practice. It would be desirable to have a reactor with a core radiation fraction of order 50%. Reactor levels of $Q_{||u}$ can be estimated by assuming a 1 cm SOL width, and that 2/3 of the power goes to the outboard divertor. Results for various reactors are shown in Table VI.

It is natural to examine if the radiation can be increased by adding impurities so that the heat flux on the divertor plate becomes tolerable. The heat flux on the divertor plate verses $Q_{||u}$ is plotted in Fig.5 for Ar. Increasing the impurities to a level corresponding to $Z_{eff} = 4$ does not lead to a large radiation fraction at reactor levels of $Q_{||u}$. For reactor profiles, $Z_{eff} \sim 4$ leads to the radiation of all the heating power in the core. Hence, with a constant impurity fraction, it is not possible to radiate much heating power in the SOL.

The preceding results have assumed a spatially uniform impurity fraction. Impurity

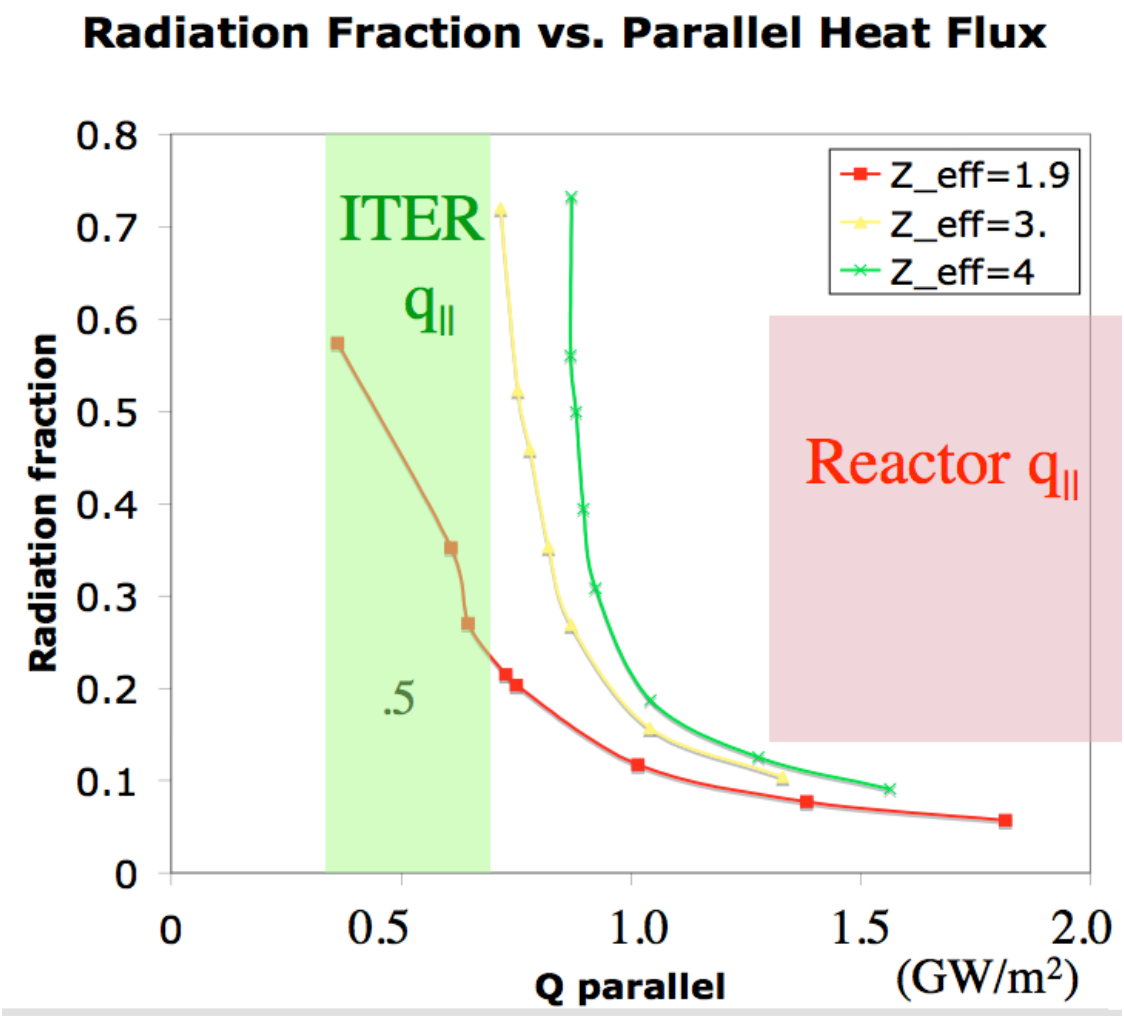

FIG. 5: Heat flux on the divertor plate verses upstream heat flux $Q_{||u}$.

entrainment does increase the amount of radiation in the divertor region without affecting the main plasma. Unfortunately, even high levels of entrainment do not enable reactor levels of $Q_{||u}$. If the concentration of impurities close to the plate is assumed to be greater than 10 times the concentration in the core plasma, then it is possible to get high radiation fractions at reactor levels of $Q_{||u}$. However, the radiation peaks very near the plate so that a large fraction of the radiated energy falls on the plate in the high heat flux region. Hence the peak heat flux from the plasma plus the radiation still exceeds 20 MW/m^2.

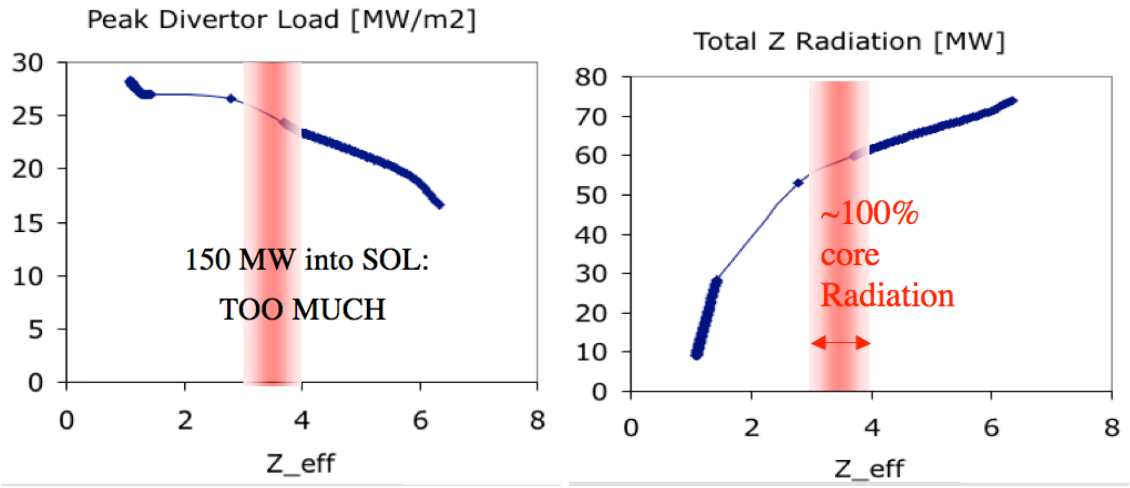

FIG. 6: Peak heat flux exceeds $10MW/m^2$, even for large core Z_{eff}, at moderate P_{SOL}.

C. Results with UEDGE

Simulations using the 2-D code UEDGE and performed in ITER-FEAT geometry confirm the conclusions drawn from the extended 1D model. For ∼100 MW into the SOL, results from B2-EIRENE [21, 22] are also essentially confirmed. With either Carbon (C) or Neon (Ne) as the impurity, a separatirx density of $\sim 0.3 \times 10^{20}$, and a core $Z_{eff} < 2$, the peak heat flux is $9 - 10MW/m^2$. Slight increases in the density lead to full detachment.

If P_{SOL} is increased even modestly, the peak heat flux exceeds 10 MW/m^2 even for large core Z_{eff}. This is shown in Fig.6 for both Carbon and Neon. For 150 MW into the SOL, increasing the level of SOL impurities does not prevent the peak heat flux from substantially exceeding$10MW/m^2$. This essentially confirms the results of the extended 1D model above-there is little benefit of increased SOL impurities above $Z_{eff} \sim 2$.

D. The potential for a radiating mantle

If it is not possible to radiate reactor power in the SOL, it must be radiated in the core. To avoid damaging the core confinement, the idea of a "radiating mantle", i.e., creating a radiating zone in a small region very close to the plasma edge, appears rather attractive. This concept has been examined in the H-mode experiments and also in the so called "RI" mode. While effective "radiating mantles" are possible on present experiments, the analysis in this section indicates that this scenario is unlikely to extrapolate to a reactor.

In plasmas without an edge transport barrier, TEXTOR has obtained extremely high f_{rad} ($\sim$ 95% of the input power) along with H-mode levels of confinement in the "RI" mode. However, it has not been possible to reproduce the equivalent on the larger and more reactor-relevant JET. This was attributed to a lack of adequate core fueling [40] - a condition that will be even more severe in a reactor. In addition, the TEXTOR RI modes has highly peaked pressure profiles [41] ($p(0)/ < p > \sim 4-5$). These peaking factors yield very poor ideal MHD stability limits. The experimental as well as theoretical analysis limit is $\beta_N \sim 2$ [42] even for shaped plasmas - well below the demands of an attractive reactor.

We now concentrate on H-mode plasmas because their much broader pressure profiles lead to higher β_N limits (with or without an ITB), and also because H-modes are the reference mode for projected ITER operation. We had already found that core radiation fraction needed in reactors with SD is $\sim$70-90% and we had also hinted it was unlikely that such a fraction can be attained in H-modes without strong confinement deterioration. Loss of confinement occurs via the following chain of events : 1) the core radiation reduces the transport power flowing through the H-mode pedestal, 2) the pedestal pressure is observed to depend on transport power in many experiments (experimental support for this conclusion is given in Appendix **??**, 3) there exists general agreement that the pedestal pressure strongly affects core confinement in experiments (also predicted by stiff ion temperature gradient [ITG] models of transport [43–45], and finally 4) a reduction in pedestal pressure with reduced transport power implies lower stored energy.

These arguments suggest that the effects of core radiation can be incorporated by following the simple rule: when the H-mode scaling laws are used to predict stored energy, the heating power should be taken to be the absorbed input heating power minus the core radiation power. The stored energy is thus effectively reduced by the factor $(1-f_{Rad,Core})^{0.31}$ (since the stored energy from the reference scaling law employed for ITER-FEAT, ITER98(y,2), scales with heating power as $P_{heat}^{0.31}$). For core radiation fractions of $< 50\%$, this results in a confinement deterioration of $< 20\%$ - an estimate consistent with experimental results. However, for a core radiation fraction of 80%, the confinement reduction is $\sim 40\%$. As noted in Sec. II, a 70% core radiation fraction may be acceptable for the H-mode reactor design, but not for advanced tokamak designs.

The preceding discussion offers a proper perspective for viewing the "radiating mantle" approach. If a substantial amount of the heating power could be radiated at the outer edge

of the pedestal (but inside the last closed flux surface), the confinement degradation could be signifiantly less than the preceding arguments would imply. The heating power would remain high in this picture in most of the pedestal because the radiation is assumed to be limited to the outer edge. If it works, the "radiating mantle" will be an attractive radiation solution. Since the pedestal region has a relatively small volume compared to the core, this scenario would demand that the radiated power density is much higher in the pedestal edge than in the plasma core. In the reminder of this section, we examine if physical mechanisms at our disposal can conspire to create such a distribution of radiation.

Line radiation in the model due to Post et. al. [46] depends on three parameters- the temperature, the ratio of the neutral DT density to the plasma density, and the product of the recycling time and the plasma density $n\tau_{recycle}$. Note that as $n\tau_{recycle}$ becomes long and the neutral density becomes small, the radiation rate approaches the value in coronal equilibrium. When $n\tau_{recycle}$ is small and the neutral density is large, the radiation can be raised above the coronal value by up to 1-2 orders of magnitude.

For coronal radiation, there is quite an unfavorable trend of the mantle radiation with rising temperature, i.e., as we go from present H-mode experiments to reactor H-modes. The possible non-coronal boost also does not help much; it scales just as unfavorably as one extrapolates from present experiments to reactors parameters because the neutral density in the plasma decreases and $n\tau_{recycle}$ increases. Our quantitative estimates reflect the qualitative reassoning; they show that the concept of a radiating mantle does not extrapolate well from present experiments to reactors with an H-mode edge.

With some simplifying assumptions (Appendix E) the magnitude of the trends mentioned above can be found easily. The main assumptions are: 1) a global particle diffusion time τ_d is used as a parameter, and 2) relationships between τ_{recyle} and the neutral density with τ_d can be deduced making reasonable assumptions about the profiles. The figure of merit for a radiating mantle is the dimensionless number R_{mantle} - it is the ratio of the radiated power in the pedestal to the radiated power in the core. If this ratio came out to be much higher than one, it would be possible to radiate a large fraction of the power in the relatively small volume of the mantle. If this ratio is of order one, then most of the radiation will necessarily come from the much large volume of the core.

Results displayed in Fig.7 reveal that R_{mantle} for an H-mode reactor (at ∼15-20 keV) is dramatically smaller than what pertains to present experiments (at ∼2 keV). The contrast

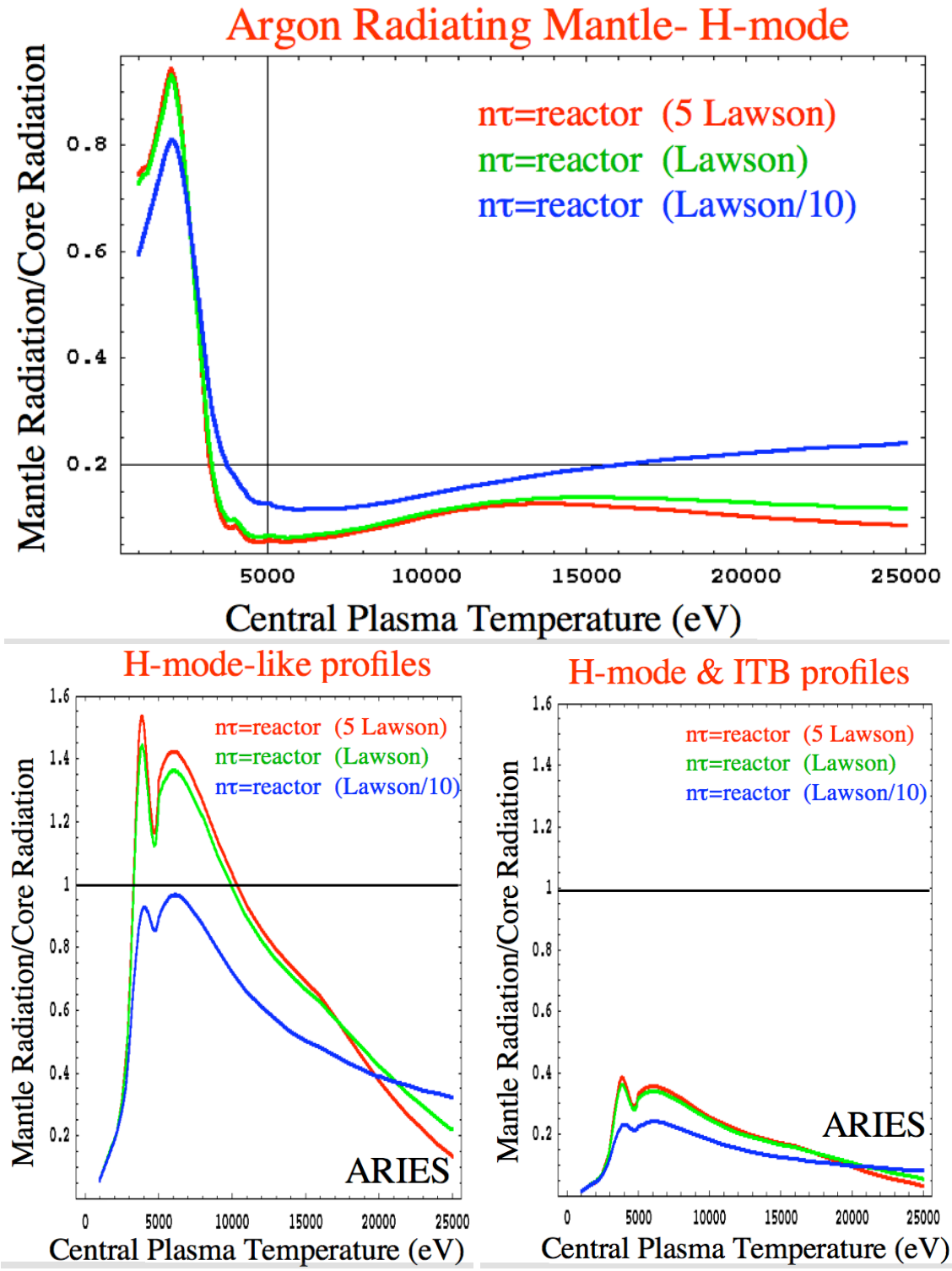

FIG. 7: The ratio R_{mantle} of the radiated power per unit volume in the pedestal to the radiated power per unit volume in the core.

is even bigger for higher and more reactor relevant $n\tau$. Radiating mantle experiments in current devices are not expected to extrapolate to a reactor with an H-mode edge.

We have now exhausted the radiation strategies; both the SOL and the radiating mantle options have been found to be inadequate for reactors although both mechanisms work well in the current machines. In Figs.4 and 7, the essence of the physics of non-extrapolatability is displayed via five dimensionless parameters (F, C, E, R, and R_{mantle}) that serve as figures of merit for the ratio of the non-core to core radiation. They all scale unfavorably from current machines to ITER and on to the regime of reactor operation.

V. ARE REACTOR ITB'S COMPATIBLE WITH STANDARD DIVERTORS?

In this section we explore whether operation in an ITB mode can provide high enough confinement needed for an SD reactor which must radiate $\sim 90\%$ of its heating power.

A. High SOL radiation with ITBs

Since an Internal Transport Barrier (ITB) is separated from the edge, it would seem possible that an ITB plasma could get good confinement without an H-mode like barrier at the edge. Without the need for an edge barrier, a fully detached plasma might be possible and such a plasma could radiate a large fraction of the power at the edge. Alternatively, a radiating mantle may be possible at the much lower edge temperatures of an L-mode edge.

The discussion in Appendix B shows that a detached plasma will have either a pedestal that is little different from an L-mode edge, or an actual L-mode edge. Experiments on DIII-D, JET, and JT-60 find that MHD beta limits are very low for ITB plasmas with an L-mode edge. The plasma disrupts due to an apparent ideal instability at $\beta_N \sim 2$ or below [47–50] - much lower than the values needed for a power reactor (or even for the proposed AT operation in ITER-FEAT). Ideal MHD stability analysis reveals that the low beta limits in L-mode ITB discharges are due to relatively strong pressure peaking[47–49]. The association of pressure peaking and low β_N is confirmed by experiments [47, 51] and analysis [52]; both show that larger β_N are obtained for plasmas with an H-mode edge (and thus broader pressure profiles) can. When pressure profiles are highly peaked, even wall stabilization causes little improvement in the accessible plasma beta [52]. The combination

of these experimental and theoretical results indicates that it is unlikely that a plasma with an L-mode edge is unlikely to have acceptable β_N, even with wall stabilization.

A reactor must have a high β_N along with good confinement. The best β_N from experiments with an L-mode edge is $\sim$ half that of the best plasmas with an H-mode edge. Given the discouraging experimental results for ITB plasmas with an L-mode edge, one concludes that reactor grade plasmas will likely require an H-mode edge, and hence fully detached plasmas are not a viable option even for ITB operations. Thus the severe limitations on the SOL radiative capacity, which forced a large core radiation fraction, pertain for an ITB operation. There is no escape from large core radiation fraction if the divertor/SOL region is not fundamentally redesigned.

The next step in the further exploration of ITBs is to investigate whether such a plasma can remain reactor-relevant if its core is highly radiating ($f_{rad-core} \sim 80 - 90\%$). If the radiation occurs in the plasma inside the ITB, it is reasonable to estimate the confinement properties by subtracting the radiation from the heating power. However, if the radiation were to occur outside the ITB, then the heating power would still flow through the ITB, and confinement might not suffer severe damage. This might be considered an example of the "radiating mantle" concept applied to ITB discharges.

The "radiating mantle" solution will be difficult to harness if the density outside the ITB is much less than the density inside the ITB. Unfortunately, a large density drop is precisely what appears to be dictated by the need for high beta and high bootstrap fraction. The qualitative argument goes as follows. High beta is required for an economically attractive fusion reactor, and is limited by ideal MHD stability limits. These stability limits are well described as a limitation on the normalized $\beta_N = \beta/(I/aB)$. Therefore, high β requires a high current, and hence a high bootstrap current. The bootstrap current is driven much more strongly by a density gradient than a temperature gradient. Therefore, for highest β values density gradients must constitute a significant fraction of the pressure gradient.

Quantitative results illustrate these points. We used the MHD equilibium code VMEC [53] with pressure profiles similar to those found on ITB experiments with high β_N. The MHD equilibria were computed for fixed β_N and with a varying ratio of density to temperature gradient. To attain beta values which are similar to those used in reactor studies, a substantial density gradient is needed in the ITB, so that the core density is over twice the edge density. The radiation power for impurities such as Ar and Kr is then calculated for

these profiles. The radiation is taken to be coronal (corrections to coronal values are estimated and found to be small, except for a very small region in the pedestal). As indicated in the section above, without any impurity accumulation within the ITB, the large majority of the radiated power comes from within the ITB. This is due primarily to the higher density there. It the impurity levels are enhanced inside the ITB, as found in experiments on JT-60U and JET [54, 55], then roughly 90% of the radiation comes from inside the ITB.

When one adds to this: a) the extreme thermal instability that the ITB discharge is prone to at high radiation fraction (see Sec.VI), and b) the possibility of core collapse from Helium build-up (see Sec.VI A), reactor operation with an ITB does not appear to provide a way out of the radiation trap imposed by the standard divertor (SD).

VI. THERMAL INSTABILITY IN A BURNING PLASMA WITH A HIGH RADIATION FRACTION

A unique feature of burning plasmas is that a high core radiation fraction $f_{rad-core}$ causes a strong thermal instability; this instability is not present in externally heated plasmas. The self-heating dynamics of such a plasma makes it prone to rapid swings in the power output. To examine the stability of the evolution equation

$$n\frac{dT}{dt} = -\frac{nT}{\tau_E} + P, \tag{13}$$

we need the temperature dependence of the heating power P= (fusion alpha power P_α + external power P_{ext} - radiation power P_{Rad}) and of the confinement time τ_E. Empirical scaling laws give τ_E as a function of the heating power P. To write the confinement time as a function of the average plasma temperature, one invokes the relation $P\tau_E$=nTV, where the volume V=$4\pi Ra^2\kappa$, R, a, and κ being the major radius, the minor radius and the elongation, respectively. For the H-mode scaling law ITER98H(y,2), the power dependence of $\tau_E \sim P^{-0.69}$ translates to a temperature dependence of $\tau_E \sim T^{-\epsilon}$, with $\epsilon = 2.2$. Temperature perturbations also change the heating power. We presume for simplicity that the shape of the temperature profile stays the same while the profile changes multiplicatively. Then, in the vicinity of a given temperature, the heating power goes as $\sim T^\alpha$. Similarly, the radiation power changes as T^ρ. Temperature perturbations can be shown to have a growth rate γ,

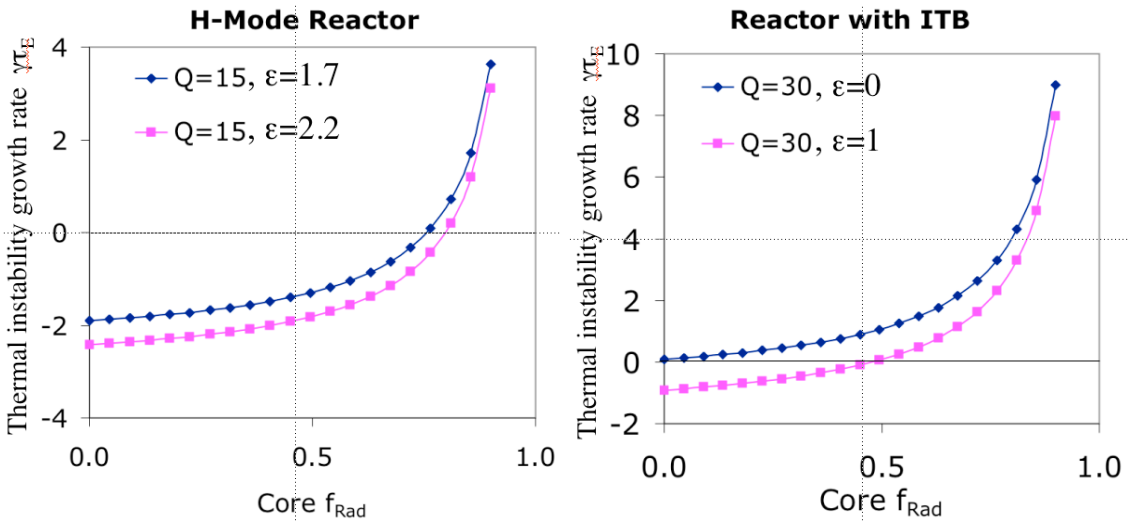

FIG. 8: Thermal instability growth rate $\gamma\tau_E$ verses core radiation fraction in a reactor with H-mode or one with ITB. The growth rate increases very rapidly beyond f_{Rad}=0.7.

which when normalized to the net energy confinement time τ_E, becomes (see Fig.8)

$$\gamma\tau_E = \frac{1}{1 - f_{Rad,Core}} \left[\frac{\alpha}{1 + 5/Q} - \rho f_{Rad,Core} \right] - (\epsilon + 1) \tag{14}$$

where Q is the external plasma heating power (assumed constant in time) divided by the total fusion energy (including that of neutrons). For H-mode like profiles and the reactor temperature of EU-B, $\alpha = 1.06$, and $\rho = 0.18$ for Argon (we have found that Argon leads to the best thermal stability, so we take the impurity to be Argon in this section).

The thermal instability growth rate is an increasing function of the radiation fraction, and the normalized growth rate becomes singular as $f_{Rad,Core}$ approaches unity. This system is stable if fusion power is negligible (Q<1, as in most present experiments). Even in an ignited plasma, the plasma is thermally stable if there is no radiation. Instability can result from increasing Q or radiation. ITER-FEAT with Q=10 and $f_{Rad,Core}$∼40% is stable. For Q=15, and $f_{Rad,Core}$∼70%, the reactors EU-A and EU-B are stable.

The thermal instability growth rate is also sensitive to the exponent in the energy confinement time. According to the empirical scaling law the exponent ϵ∼2. However, for ITB discharges in JET the stored energy varies more strongly with input power than in the case of H-modes, implying a stronger thermal instability. With low central magnetic shear, the stored energy varies roughly as $P^{0.5}$, corresponding to ϵ=1 [56]. For JET reverse shear (RS) discharges the stored energy varies nearly linearly with the heating power P, or ϵ∼0 [57].

Advanced tokamak reactor studies (e.g. ARIES-RS, EU-C, and CREST) have $T{\sim}16$ keV. For profiles with a broad pressure and ITB, this leads to $\alpha = 0.95$ and $\rho = 0.19$. The Q for these studies is ~ 30.

Advanced tokamak (AT) scenarios envisaged for ITER have much lower $Q{\sim}5$, and much lower core radiation fractions. Within the framework of this model, such discharges are expected to be thermally stable. Hence, ITER-FEAT will be unlikely to test the thermal instability characteristics of ITB scenarios which will arise in a reactor with an SD.

For ITB based reactors, the model predicts severe thermal instability in the relevant range of $f_{rad-core}$ with growth rates 1.3-6 times the energy confinement time. It is probably not possible to control such a virulent instability using feedback on the impurity puffing, or fueling - these signals do not propagate into the core quickly enough. Only the feedback on the external heating power might be fast enough, but this becomes progressively less robust at high Q, since the control signal has a small dynamic range. By increasing the power capacity of the divertor by merely a factor of ∼2-3, it is possible to stabilize the thermal instability, or at least slow its growth time to values longer than the confinement time so that impurity puffing or fueling can be used for feedback. These controls have a much larger dynamic range imparting them the necessary robustness. The new X-divertor (XD) proposed and described in Sec.III increases the divertor power capacity to this range.

In a plasma with $\sim 90\%$ radiation, a small perturbation in fusion power will lead to a much larger change in the net power $(P_\alpha - P_{rad})$ onto the divertor plate since the radiation does not increase commensurately with perturbations. For an ITB reactor with a high radiation fraction, the doubling time of power on the plate would be a fraction of one second. For a divertor plate close to the engineering limit, a short transient could cause damage requiring replacement (months of downtime). Thus, a crucial requirement for such a reactor is to demonstrate very effective stabilization of the thermal instability under all perturbing conditions that affect heating and radiation balance. Such perturbations could be: 1) routine and expected such as pellet injection and ELMs, or 2) sporadic occurrences like flakes falling into the plasma, or 3) off-normal events such as equipment transients and failures. In principle such swings can perhaps be detected and feedback stabilized. The swing control, however, can become much more difficult as the ratio of the heating to the fusion power becomes lower (i.e. Q becomes higher, as it must in an attractive reactor).

Thus if ITER-FEAT were to demonstrate the physics performance necessary for a power

reactor, it must access and explore this thermally unstable range, and also demonstrate the feasibility of a robust scheme for feedback stabilization. However, it will not have an H-mode at $f_{Rad} > 60\%$ and cannot access and study strong alpha heating and core thermal instability - precisely the regimes critically relevant to an SD reactor.

There are other serious physics consequences of the core thermal instability. Because of its tendency to induce large power swings into the SOL, any modest drop in input power to a highly radiating SOL may cause an SOL radiation collapse into full detachment. This, in turn, will cause a drop in core confinement, leading to a further loss of fusion power. The system may not recover from this vicious cycle, ending in a disruption or emergency shutdown. The thermal instability (caused by a high radiation fraction in the core - a necessity for an SD reactor) and its consequences should give us pause. A highly thermally unstable core plasma coupled to a highly radiating SOL is a novel complex physical system with much potential for disruption; it will be of questionable practicality, especially in a radioactive reactor setting subject to strong regulations.

Operating a reactor in a highly thermally unstable plasma regime is most probably unacceptable. The core radiation fraction required to save the divertor, therefore, must fall below the threshold for thermal instability or at least fall enough that the thermal instability becomes weak. What we need, then, is to design and test divertors that can handle significantly more power than the standard divertors used on current and proposed machines; the need for the X-divertor is even greater than what we had anticipated.

A. Helium build-up - Core radiation collapse

Even if it were somehow possible to obtain high enough confinement in highly radiating ITB's, the plasma transport will be too low for adequate helium exhaust - the result will be a radiation collapse of the core inside the ITB. To analyze this situation, we build a model similar to that of Wade et al. [35]. Assuming the temperature, and electron and impurity density profiles pertinent to an ITB reactor, the fusion heating and radiation power can be computed from known cross sections. The heat diffusivity χ, consistent with the profiles and the net heat fluxes, can then be derived. The source of helium from fusion can also be computed. To compute helium density, one needs appropriate transport coefficients. The first step in this direction is provided by the experimental findings [58] that the helium

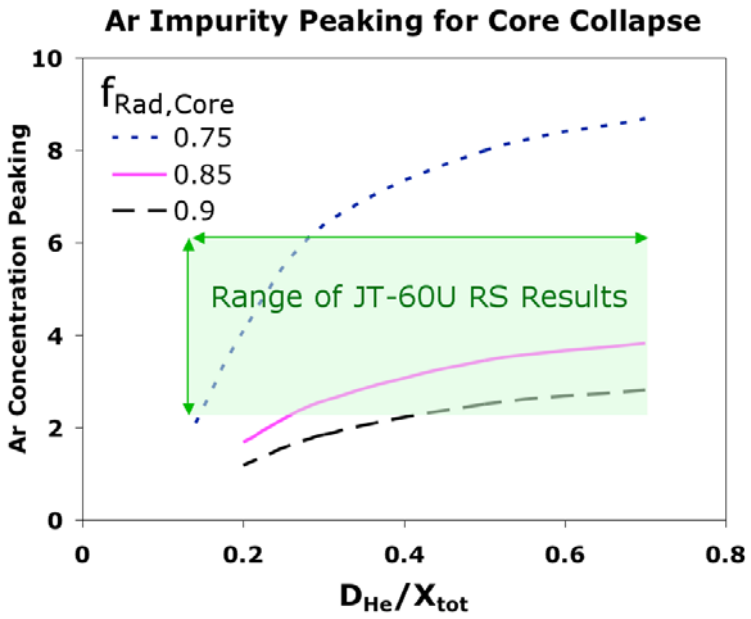

FIG. 9: Maximum tolerable impurity density (Ar) peaking verses helium diffusivity.

diffusivity in H-modes is roughly 0.7 times the total heat diffusivity, and the helium pinch is the same as the density pinch. We use these results in the region outside the ITB. For inside the ITB, we assume purely diffusive helium transport, motivated by the JT-60U [54] result that the helium diffusivity inside the ITB is determined to be between $0.2 - 1.0$ times the ion heat diffusivity (and the helium pinch in the ITB is assumed zero). The ion heat flux is about $\sim$ 70% of the total heat flux. These results allow the helium density to be determined via a 1D transport analysis.

For a sufficiently low helium diffusivity, the helium in the core builds up until the radiation rate inside the ITB exceeds the decreasing fusion heating rate, and there is no solution. In practice, a core radiation collapse would occur. The maximum tolerable impurity peaking before the radiation collapse naturally depends on helium diffusivity. The maximum impurity peaking is plotted versus helium diffusivity in Fig.9. For core radiation fractions $f_{rad-core} \sim 85\%$, most of the existing experiments lie in the range of radiation collapse. For $f_{rad-core} \sim 70\%$, most of the data is outside the range for radiation collapse. On the basis of extrapolations of existing data, we conclude that at core radiation fractions $\sim 85\%$, there exists a substantial possibility of core collapse due to Helium buildup in ITB discharges.

VII. CONCLUSIONS

We find that the standard divertor SD (used in current and proposed machines), with its limited heat-handling capability, emerges as an unacceptably weak link in the chain leading to a dependable and economic power reactors. The low heat rating of SD mandates an extremely high radiation fraction in the plasma, which in turn has devastating effects on the core confinement and stability of a burning plasma. In the main text and in the appendices, we have shown that present experimental experience and theoretical arguments imply that a reactor employing the standard divertor (SD) cannot have acceptable confinement and β at the same time, and will have a high risk of thermal instability and disruptions. These conclusions apply to operation with ITBs as well as H-modes.

Solving the thermal exhaust problem without placing an unbearably high radiation burden on the plasma core thus emerges as one of the most fundamental challenges of reactor physics. The obvious solution would be to place a part of the radiation elsewhere; in the SOL or in a thin mantle at the edge of the core. Both these radiation strategies were examined (drawing on experimental data and a variety of codes) and found to be inadequate for reactor power levels even though there is evidence that they work well at low power levels characteristic of the present experiments. At power levels peculiar to reactors, the atomic physics and the nature of the parallel transport conspire so that none neither the SOL nor a mantle can handle a large enough fraction of the total radiation. Any mechanism that we invoke to enhance the SOL or the mantle share ends up preferentially enhancing the core radiation fraction. The essence of the physics of non-extrapolatability is captured by five dimensionless parameters that serve as figures of merit (F, C, E, R, and R_{mantle}). All of them scale unfavorably from current machines to the regime of reactor operation.

Having failed to find a radiation solution, the challenge of reducing f_{rad} down to a manageable level shifts to somehow increasing the thermal rating of the divertor. We do this by proposing to modify the magnetic geometry of the divertor. By creating an X-point near the divertor plate, the magnetic field in the open field line region is flared to increase the area over which the heat is spread. This new configuration (called the X-divertor or XD) along with acceptable magnetic equilibria can be created with coils that may be located behind neutron shields. The desired geometry is accessible with fairly moderate currents in the additional coils. The resulting increase in the plasma-wetted area considerably re-

duces the amount of required radiation before the thermal flux hits the divertor plate. The X-divertor, described and explained in Sec.III, brings the required radiation fraction (for a high power reactor) much closer to the range where ITER-FEAT is expected to operate. As an additional bonus, the lower poloidal fields of the XD geometry will enable liquid metal divertors [15–17] with an even higher heat flux capacity.

By reducing the radiation fraction to manageable levels, the new X-divertor could vastly reduce the requirements on core confinement. In fact, confinement times less than the ones predicted by H-mode scaling laws can suffice for some reactor designs. Within the class of machines using the new X-divertor, one could then confidently extrapolate to reactors the results obtained on relatively low power burning plamas.

Since the divertor part of the magnetic bottle assumes immense and critical importance as one approaches reactor power levels (it controls the behavior of the plasma core), much attention must be paid to the design, construction and testing of divertors with heat capacity much larger than the standard divertor. The new X-divertor presented in this paper can serve as a representative of this class. The XD also opens the possibility of an attractive route to fusion through the following possible steps : 1) Test the XD by modifying one or more of the current machines, 2) build a modest cost and size copper based burning plasma experiment, but with the new XD. We have found nothing that will prevent this experiment from laying the groundwork for a Component Test Facility (CTF), and demonstrating the crucial physics for a credible fusion reactor. In fact, both the power and Q of such a device can be raised by simply making it larger (relying on the most dependable trend in past 30 years of fusion research), 3) build a CTF. It is possible that (2) and (3) could be combined into a single step, and finally 4) design a demonstration XD fusion reactor (DEMO) by simply making the machine bigger and more powerful.

VIII. ACKNOWLEDGMENTS

We gratefully acknowledge help from M. Pekker. This work was supported by ICC Grants from US DOE.

* Email:pvalanju@mail.utexas.edu

[1] G. Marbach, I. Cook, and D. Maisonnier, Fusion Eng. Des. **63-64**, 1 (2002).

[2] F. Najmabadi and the ARIES Team, Fusion Eng. Des. **38**, 3 (1997).

[3] K. Okano, Y. Asaoka, T. Yoshida, M. Furuya, K. Tomabechi, Y. Ogawa, N. Sekimura, R. Hiwatari, T. Yamamoto, T. Ishikawa, et al., Nucl. Fusion **40**, 635 (2000).

[4] D. J. Campbell, Phys. Plasmas **8**, 2041 (2001).

[5] J. Connor, T. Fukuda, X. Garbet, C. Gormezano, V. Mukhovatov, M. Wakatani, the ITB Database Groupa, the ITPA Topical Group on Transport, and I. B. Physics, Nucl. Fusion **44**, R1 (2004).

[6] E. J. Synakowski, Plasma Phys. Control. Fusion **40**, 581 (1998).

[7] Editors, Nuclear Fusion **39**, 2137 (1999).

[8] A. S. Kukushkin, H. D. Pacher, G. Federici, G. Janeschitz, A. Loarte, and G. W. Pacher, Fusion Eng. Des. **65**, 355 (2003).

[9] V. Mukhovatov, M. Shimada, A. N. Chudnovskiy, A. E. Costley, Y. Gribov, G. Federici, O. Kardaun, A. S. Kukushkin, A. Polevoi, V. D. Pustovitov, et al., Plasma Phys. Control. Fusion **45**, A235 (2003).

[10] I. P. E. G. on Divertors, Nuclear Fusion **39**, 2391 (1999).

[11] A. S. Kukushkin, H. D. Pacher, G. W. Pacher, G. Janeschitz, D. Coster, A. Loarte, and D. Reiter, Nucl. Fusion **43**, 716 (2003).

[12] I. Cook, N. Taylor, D. Ward, L. Baker, and T. Hender, Tech. Rep. 521, UKEA FUS, Euratom/UKEA Fusion Association (2005).

[13] M. Sato, S. Sakurai, S. Nishio, K. Tobita, T. Inoue, Y. Nakamura, K. Shinya, and H. Fujieda, Fusion Eng. Des. **81**, 1277 (2006).

[14] I. Cook, N. P. Taylor, and D. J. Ward, in *Proceedings of the Symposium on Fusion Engineering* (San Diego, 2003).

[15] M. Narula, A. Ying, and M. A. Abdou, Fusion Science and Technology **47**, 564 (2005).

[16] M. Abdou, N. Morley, T. Sketchley, R. Woolley, J. Burris, R. Kaita, P. Fogarty, H. Huang, X.Lao, M. Narula, et al., Fusion Engineering and Design **72**, 35 (2004).

[17] X. Zhou and M. S. Tillack, Tech. Rep. UCSD-ENG-079, University of California, San Diego (1998).

[18] M. A. Abdou, Fusion Engineering and Design **27**, 111 (1995).

[19] P. Norajitra, R. Giniyatulin, T. Ihli, G. Janeschitz, P. Karditsas, W. Krauss, R. Kruessmann,

V. Kuznetsov, D. Maisonnier, I. Mazul, et al., in *IAEA FT/P7-13* (2004).

[20] S. J. Zinkle, National Academy of Engineering publications **28** (1998).

[21] B. Braams, Tech. Rep. (NET) EUR-FU/XII-80/87/68, Comm. of the EC, Brussels (1987).

[22] D. Reiter, Tech. Rep. 2599, Institut für Plasmaphysik, Association EURATOM-KFA (1992).

[23] A. Garofalo, E. Doyle, J. Ferron, C. Greenfield, R. Groebner, A. Hyatt, G. Jackson, R. Jayakumar, J. Kinsey, R. L. Haye, et al., Phys. Plasmas **13**, 056110 (2006).

[24] A. Isayana and the JT-60 Team, Phys. Plasmas **12**, 056117 (2005).

[25] T. Fujita and the JT-60 Team, Phys. Plasmas **13**, 056112 (2006).

[26] D. P. Coster, in *Proceedings of 10th International Toki Conference on Plasma Physics and Controlled Nuclear Fusion* (Toki-city Japan, 2000), pp. 1–5.

[27] P. C. Stangeby, *The Plasma Boundary of Magnetic Fusion Devices* (IOP Publishing Ltd, 2000).

[28] W. Fundamenski, S. Sipil, and J.-E. contributors, Nucl. Fusion **44**, 20 (2004).

[29] M. T. Kotschenreuther, P. M. Valanju, and S. M. Mahajan, in *Proceedings of the 20th International Conference on Fusion Energy* (Vilamoura Portugal, 2004).

[30] M. T. Kotschenreuther, P. M. Valanju, and S. M. Mahajan (2004), submitted to Fusion Engineering Design.

[31] A. S. Kukushkin, H. D. Pacher, G. Janeschitz, A. Loarteb, D. Costerc, and D. Reiterd, in *Proceedings of the 28th EPS conference on Controlled Fusion and Plasma Physicsth EPS Conference on Controlled Fusion and Plasma Physics* (Funchal, 2001).

[32] A. S. Kukushkin, H. D. Pachera, G. Janeschitz, D. Costerb, D. Reiterc, and R. Schneider, in *Proceedings of the 26th EPS Conference on Controlled Fusion and Plasma Physics* (Maastricht, 1999), vol. 231, pp. 1545–1548.

[33] D. Strickler, in *Proceedings, IEEE Thirteenth Symposium on Fusion Engineering* (1990), p. 898.

[34] A. W. Leonard, M. A. Mahdavi, S. L. Allen, N. H. Brooks, M. E. Fenstermacher, D. N. Hill, C. J. Lasnier, R. Maingi, G. D. Porter, T. W. Petrie, et al., Phys. Rev. Lett. **78**, 4769 (1997).

[35] M. R. Wade, W. P. West, R. D. Wood, S. L. Allen, J. A. Boedo, N. H. Brooks, M. E. Fenstermacher, D. N. Hill, J. T. Hogan, R. C. Isler, et al., J. Nucl. Mater. **266-269**, 44 (1999).

[36] J. Rapp, T. Eich, M. von Hellerman, A. Herrmann, L. Ingesson, S. Jachmich, G. Matthews,

V. Saibene, and contributors to the EFDA-JET Workprogramme, Plasma Phys. Control. Fusion **44**, 639 (2002).

[37] H. Kubo, S. Sakurai, N. Asakura, S. Konoshima, H. Tamai, A. Sakasai, H. T. enaga, K. Itami, K. Shimizu, T. Fujita, et al., Nucl. Fusion **41**, 227 (2001).

[38] R. Clark, J. Nucl. Mater. **220-222**, 1028 (1995).

[39] J. A. Boedo, G. D. Porter, M. J. Schaffer, R. D. Lehmer, R. A. Moyer, J. G. Watkins, T. E. Evans, C. J. Lasnier, A. W. Leonard, and S. L. Allen, Phys. Plasmas **5**, 4305 (1998).

[40] G. Maddison, M. Brix, R. Budny, M. Charlet, and I. Coffey, Nucl. Fusion **43**, 49 (2003).

[41] D. Kalupin, P. Dumortier, A. Messiaen, J. Ongena, B. Unterberg, R. Weynants, R. Jaspers, R. Koslowski, G. Mank, and G. V. Wassenhove, in *Proceedings of the 27th EPS Conference on Controlled Fusion and Plasma Physics* (Budapest, 2000), vol. 24B, pp. 1417–1420.

[42] H. R. Koslowski, G. Fuchsa, R. Jaspersb, A. Kramer-Fleckena, A. Messiaen, , J. Ongenac, , J. Rappa, F.C.Schullerb, et al., Nucl. Fusion **40**, 821 (2000).

[43] M. T. Kotschenreuther, W. Dorland, Q. P. Liu, G. W. Hammett, M. A. Beer, S. A. Smith, A. Bondeson, and S. C. Cowley, in *Proceedings of the 16th IAEA Fusion Energy Conference* (Montreal, Canada, 1996).

[44] R. E. Waltz, G. M. Staebler, W. Dorland, G. W. Hammett, M. Kotschenreuther, , and J. A. Konings, Phys. Plasmas **4**, 2482 (1997).

[45] J. E. Kinsey, in *Proceedings of the 19th International Conference on Fusion Energy* (Vilamoura Lyon, 2002).

[46] D. Post, J. Abdullah, R. Clark, and N. Putvinskaya, Phys. Plasmas **2**, 2328 (1995).

[47] E. A. Lazarus, G. A. Navratil, C. M. Greenfield, E. J. Strait, M. E. Austin, K. H. Burrell, T. A. Casper, D. R. Baker, J. C. DeBoo, E. J. Doyle, et al., Phys. Rev. Lett. **77**, 2714 (1996).

[48] A. Sips and the JET Team, Nucl. Fusion **41**, 1559 (2001).

[49] T. Fujita, Y. Kamada, S. Ishida, Y. Neyatani, T. Oikawa, S. Ide, S. Takeji, Y. Koide, A. Isayama, T. Fukuda, et al., Nucl. Fus. **39**, 1627 (1999).

[50] S. Takeji, S. Tokuda, T. Fujita, T. Suzuki, A. Isayama, S. Ide, Y. Ishii, Y. Kamada, Y. Koide, T. Matsumoto, et al., Nucl. Fusion **42**, 5 (2002).

[51] A. C. C. Sips, E. J. Doyle, C. Gormezano, Y. Baranov, E. Barbato, R. Budny, P. Gohil, F. Imbeaux, E. Joffrin, T. Fujita, et al., in *Proceedings of the 20th International Conference on Fusion Energy* (Vilamoura, Portugal, 2004), pp. 1–8.

[52] A. D. Turnbull, T. S. Taylor, M. S. Chu, R. L. Miller, and Y. R. Lin-Liu, Nucl. Fusion **38**, 1467 (1998).

[53] S. P. Hirshman and J. C. Whitson, Phys. Fluids **26**, 3553 (1983).

[54] H. Takenaga, Nucl. Fusion **43** (2003).

[55] R. Dux, C. Giroud, K. Zastrow, and J. E. contributors, Nucl. Fusion **44**, 260 (2004).

[56] P. Buratti and the JET Team, in *Proceedings of the 18th International Conference on Fusion Energy* (Sorrento Italy, 2000).

[57] C. D. Challis, X. Litaudon, G. Tresset, Y. F. Baranov, A. Becoulet, C. Giroud, N. C. Hawkes, D. F.Howell, E. Joffrin, P. J. Lomas, et al., Plasma Phys. Control. Fusion **44**, 1031 (2002).

[58] M. R. Wade, T. C. Luce, and C. C. Petty, Phys. Rev. Lett. **79**, 419 (1997).

[59] V. Mertens, K. Borrass, J. Gafert, M. Laux, J. Schweinzer, and A. U. Team, Nucl. Fusion **40**, 1836 (2000).

[60] J. Rapp, A. Huber, L. C. Ingesson, S. Jachmich, G. F. Matthews, V. Philipps, R. Pitts, and C. to the EFDA-JET work programme, J. Nucl. Mater. **313-316**, 524 (2002).

[61] R. Maingi, M. A. Mahdavi, T. W. Petrie, L. R. Baylor, T. C. Jernigan, R. J. L. Haye, A. W. Hyatt, M. R. Wade, J. G. Watkins, and D. G. Whyte, J. Nucl. Mater. **266-269**, 598 (1999).

[62] A. V. Chankin, K. Itami, and N. Asakura, Plasma Phys. Control. Fusion **44**, A399 (2002).

[63] G. M. McCracken, R. D. Monk, A. Meigs, L. Horton, L. C. Ingesson, J. Lingeretat, G. F. Matthews, M. G. OMullane, R. Prentice, M. F. Stamp, et al., J. Nucl. Mater. **266-269**, 37 (1999).

[64] W. Suttrop, V. Mertens, H. Murmann, J. Neuhauser, J. Schweinzer, and A.-U. Team, J. Nucl. Mater. **266-269**, 118 (1999).

[65] M. A. Mahdavi, T. H. Osborne, A. W. Leonard, M. S. Chu, E. J. Doyle, M. E. Fenstermacher, G. R. McKee, G. M. Staebler, T. W. Petrie, M. R. Wade, et al., Nucl. Fusion **42**, 52 (2002).

[66] T. W. Petrie, S. L. Allen, T. N. Carlstrom, D. N. Hill, R. Maingi, D. Nilson, M. Brown, D. A. Buchenauer, T. E. Evans, M. E. Fenstermacher, et al., J. Nucl. Mater. **241-243**, 639 (1997).

[67] T. W. Petrie, in *Proceedings of the 28th EPS conference on Controlled Fusion and Plasma Physics* (Madiera, Portugal, 2001).

[68] S. Konoshima, H. Tamai, Y. Miura, S. Higashijima, H. Kubo, S. Sakurai, K. Shimizu, T. Takizuka, Y. Koide, T. Hatae, et al., J. Nucl. Mater. **313–316**, 888 (2003).

[69] A. Loarte, R. D. Monk, J. R. Martin-solis, D. J. Campbell, A. V. Chankin, S. Clement, S. J.

Davies, J. Ehrenberg, S. K. Erents, and H. Y. Guo, Nucl. Fusion **38**, 331 (1998).

[70] J. W. Hughes, D. A. Mossessian, A. E. Hubbard, B. LaBombard, and E. S. Marmar, Phys. Plasmas **9**, 3019 (2002).

[71] A. E. Hubbard, A. E. Hubbard, B. Lipschultz, D. Mossessian, R. L. Boivin, J. A. Goetz, R. S. Granetz, M. Greenwald, I. H. Hutchinson, D. J. J. Irby, et al., in *Proceedings of the 26th EPS Conference on Controlled Fusion and Plasma Physics* (Maastricht, 1999), pp. 13–16.

[72] F. Ryter, A. Stabler, and G. Tardini, Fusion Science and Technology **44**, 618 (2003).

[73] T. Onjun, A. H. Kritz, G. Bateman, V. Parail, H. Wilson, J. Lonnoroth, G. Huysmans, and A. Denestrovskij, Physics of Plasmas **11**, 1469 (2004).

[74] Y. Kamada, H. Takenaga, H. Urano, T. Takizuka, T. Hatae, and Y. Miura, in *IAEA-CN-94 / EX / P2-04* (2002).

[75] P. Snyder (2006), private communications.

APPENDIX A: COMPONENT TEST FACILITY (CTF) WITH XD

A Component Test Facility (CTF) [18] is recognized as a critical intermediate step for developing the fusion technology necessary for a reactor DEMO and certifying the performance of large components under high heat flux and neutron fluence. Obviously, to be useful and relevant, CTF should be significantly smaller (and cheaper) than a DEMO.

We now show that such a CTF is not realizable with a standard divertor (SD). In order to be small and low cost as compared to a DEMO, a CTF must have low Q$\sim$1. In order to be useful, it must also have a neutron wall loading $\sim$ 1-2 MW/m^2. So a CTF will have a P/R about the same as a reactor, and the survival of the standard divertor would require that most of the heating power be radiated from the plasma to the wall of the main chamber (outside the divertor). For a Q$\sim$1 CTF, the heat flux to the first wall must be the same as the neutron power flux $\sim$1-2 MW/m^2, since the injected heating power roughly equals the neutron power. However, most US and Japan reactor designs [2, 3] limit the first wall loading to less than 1 MW/m^2 and the EU designs [1] limit it to below 0.5 MW/m^2 (outside the divertor). Thus, a Q$\sim$1 CTF is not possible within engineering limits if most of the power is radiated to the first wall.

The only option for a CTF-SD (a CTF with the standard divertor) is to make it large enough that Q becomes substantially larger than 1. Together with the requirement for a large neutron wall loading, this makes a CTF-SD about as big, powerful and costly as a DEMO - only consistent with a strategy of jumping directly from ITER-FEAT to a DEMO. The risks of a DEMO failure, development delay and cost overruns are severe in this approach. Only a divertor that can withstand enough power to reduce the required radiation fraction to acceptable levels can enable operation of a small CTF with Q$\sim$1. The new X-divertor (XD) is well suited for this task. We call a CTF with XD a CTF-XD.

In addition to providing crucial engineering data, a CTF-XD that has about the same P/R as a reactor will also directly demonstrate reliable steady state power handling at reactor relevant values (the most critical engineering problem in fusion). It will also enable development components for reliable operation in a high DT neutron fluence (the other critical engineering problem in fusion). Although a CTF-XD will not demonstrate energy gain, it will lend itself to a reliable and straightforward extrapolation to a reactor. The ability of the new X-divertor (XD) to handle higher thermal power enables us to increase Q

by simply making the device bigger in size and power the historically proven reliable path for a steep climb in the Lawson parameter over the past 30 years.

APPENDIX B: FULL DETACHMENT- NOT A REACTOR OPTION

The deleterious effects of full divertor detachment from plasma (this state does enable high radiation in the SOL) are uniformly observed in currently operating machines. In ASDEX, the H-L back transition "virtually coincides with the achievement of complete detachment" [59], but on JET, the H-L back transition can occur while the inner divertor stays attached [60]. On DIII-D, "outboard divertor detachment is almost always accompanied by an H-L confinement transition" [61]. In JT-60U, H-mode could be obtained with full detachment, but the energy confinement was about that of an L-mode [62].

Completely detached plasmas on JET have poor confinement, H89P$<$1.5 [63]. On ASDEX, detachment coincides with a reduction in the edge pressure gradient [64]. Virtually all reactor designs operate above the Greenwald density limit, but on DIII-D, for discharges above the Greenwald limit, "a key step in accessing high densities without confinement degradation is prevention of a cold radiating zone at the x-point $\cdots$ correlated with detachment" [65]. This is also true on DIII-D below the Greenwald limit [66], and the degree of divertor closure does not significantly affect this [67]. However, JT-60U observes poor confinement near the Greenwald limit whether there is an X-point MARFE or not [68]. On TCV, density ramps are disruptively terminated by an X-point MARFE. In high density experiments on JET, full detachment could not be achieved without a disruption [69].

Reactors surely require confinement substantially better than L-mode [1–3, 14]. Also, no power reactor can be expected to safely operate in regimes where the probability of disruptions is anything but extremely low. The ITER physics basis [7] concludes that operation with divertor detachment leads to confinement degradation. Based on such experimental results, ITER divertor studies correctly exclude the full divertor detachment regime from consideration for H-mode operation [8]. Another study concludes that operation in steady state requires avoiding complete detachment, which usually leads to formation of an X-point MARFE and a disruptive density limit [26].

Together, these experiments indicate that fully detached operation is not acceptable for a reactor, even though fully detached operation potentially allows large amounts of power

dissipation in the SOL.

APPENDIX C: THE EXTENDED 1D MODEL

The extended 1D model is based on equations found in Stangby[27]. The ion and electron heat fluxes are defined as

$$Q_{||e} = \kappa_e \frac{dT_e}{dl} + \frac{5un_eT_e}{2} \tag{C1}$$

$$Q_{||i} = \kappa_i \frac{dT_i}{dl} + \frac{5un_iT_i}{2} + m_i n_i u^3/2 \tag{C2}$$

where the convection velocity u is an assumed function which is maximum at the plate, and decays upstream. The fluxes obey

$$dQ_{||e}/dl = f_z n^2 L_z(T) + R_H + E_{ei} \tag{C3}$$

$$dQ_{||i}/dl = -E_{ei} \tag{C4}$$

Where n_e (n_i) and T_e (T_i) are respectively the electron (ion) density and temperature, and $E_{ei} = 3(m_e/m_i)\nu_e n_e(T_i - T_e)$ is the classical term for energy exchange between electrons and ions. The heat flux is reduced by hydrogenic ionization radiation R_H, and by the radiation from a given fraction of impurities f_z which radiate with a characteristic radiation rate L_z. The flow speed u has the form

$$n_e u = F_0 exp\left[\frac{l_{plate} - l}{\lambda}\right] - F_1 \tag{C5}$$

where l, the distance along the field line, is measured from the upstream position (l=0), and l_{plate} denotes the location of the plate. The value of F_0 is set by the sheath boundary condition at l=l_{plate}, and F_1 is determined by the condition that the flow vanish at the upstream position. The density is found from the parallel momentum equation

$$m_i n_i u^2 + n_e T_e + n_i T_i = constant \tag{C6}$$

where the constants are set by the upstream values.

It will be simplest to assume the impurity density to be constant. To allow for the possibility of impurity entrainment, however, we add a contribution that could strongly increase the impurity density near the plate. Since the impurity entrainment is due to the flow which drags the impurities to the plate, the increased density of the impurities is

assumed to occur on the same scale as the flow. From these considerations, the impurity concentration f_z is taken to be

$$f_z = f_{z0} + f_{z-entrain} exp\left[\frac{l_{plate} - l}{\lambda}\right] \tag{C7}$$

APPENDIX D: DEPENDENCE OF THE PEDESTAL ON INPUT POWER

Numerous experimental results show that the pedestal pressure is sensitive to heating power P. In C-mod, the pedestal height is found to vary roughly as $\sim P^{0.5}$ [70]. The total stored energy was almost linearly proportional to the pedestal pressure. Impurity radiation has also been found to strongly reduce pedestal height on C-mod [71]. A large database of ASDEX discharges [72] shows a somewhat weaker power scaling for the pedestal $\sim P^{0.2}$. The temperature profiles were found to be stiff in this data, with core temperatures multiplicatively related (approximately) to the edge temperature. In this same data set, the stored energy scaled slightly more strongly with power than the pedestal pressure, as $\sim P^{0.28}$, when using similar regression variables. Controlled parameter scans of type I ELM discharges on JET [73], where only the power is varied, find that the pedestal pressure roughly varies as $\sim P^{0.5}$, but core confinement has a weaker power scaling. For type I ELM discharges on JT-60U with high triangularity > 0.2 and high poloidal β [74], the pedestal pressure varies with input power similar to the total stored energy (not true for low triangularity). For JET ITB shots, the pedestal pressure and the thermal stored energy were both roughly linearly proportional to the heating power (but the temperature profiles were not stiff) [57]. On DIII-D, the pedestal pressure can saturate with power for heating powers well past the H-L threshold; the pedestal depends on power only in the type III ELM regime [75]. We note that reactors with core radiation fractions $\sim 85\%$ are rather close to the threshold, and so again we would expect a dependence of the pedestal on the heating power. Hence, the data clearly support a dependence of the pedestal on power.

APPENDIX E: RADIATING MANTLE CALCULATION DETAILS

Consider a thin radiating mantle near the edge with a width δx. For simplicity, the plasma is taken to be cylindrical with an average minor radius a_{avg} and major radius R_{major}.

Let τ_d denote a characteristic global diffusion time. If the diffusion coefficient were fairly uniform throughout the plasma, the diffusion time through the mantle τ_m would roughly satisfy $\tau_m \sim \tau_d(a/\delta x)^2$. However, in an H-mode plasma, if the mantle were inside the pedestal, the local diffusion coefficient would be much smaller than the global estimate. Consequently the H-mode mantle diffusion time τ_{m-H} is much longer. For an H-mode, most of the global particle confinement comes from the edge transport barrier, so it can be shown that $\tau_{m-H} \sim \tau_d$. For an H-mode, the recylcing time $\tau_{recycle}$ will be estimated as τ_{m-H}.

$$n_{core}\tau_{recycle} = n_{core}\tau_m \tag{E1}$$

Since the particle confinement time is typically several times the energy confinement time, $n_{core}\tau_m$ should be several times the Lawson criterion for a reactor. As one goes from present experiments to reactors, $n_{core}\tau_m$ is expected to increase considerably pushing the radiation power closer to its value in coronal equilibrium.

The level of neutrals present in the pedestal can be estimated as follows. Suppose the particle source fueling the plasma comes from ionization of neutrals in the pedestal. (If there is pellet or neutral beam fueling, the neutral density in the mantle will be less, resulting in a lower neutral density, and lower mantle radiation- hence this assumption is optimistic for a radiating mantle.) Particles are lost by diffusion through the barrier at a rate Vn_{core}/τ_{m-H}, where $V = 2\pi^2 a_{avg}^2 R_{major}$ is the plasma volume and n_{core} is the typical core plasma density. Reactors operate in steady state, so the source of plasma particles from ionization S_{ion}must balance this loss. If a neutral in the pedestal has an ionization rate $\sigma v n_{ped}$, then the total number of neutrals N_{neut} must satisfy $N_{neut}n_{core}\sigma v = Vn_{core}/\tau_{m-H}$. Since the volume of the thin mantle is approximately $4\pi^2 a_{avg}R_{major}$, the ratio of the neutral density to the plasma density is

$$\frac{n_{neut}}{n_{core}} = \frac{a_{avg}}{2\sigma v \delta x n_{core}\tau_m} \tag{E2}$$

Note that the neutral ratio is considerably smaller for reactors as compared to present experiments, so the radiation power is expected to be closer to the coronal equilibrium value.

These equations are used to produce Fig.7.